Contents

Chapter 26

Relativistic Stars and Black Holes

Version 1225.1.K.pdf, 7 September 2012

Please send comments, suggestions, and errata via email to kip@caltech.edu or on paper to Kip Thorne, 350-17 Caltech, Pasadena CA 91125

Box 26.1
Reader's Guide

- This chapter relies significantly on
    - Chapter 2 on special relativity.
    - Chapter 23, on the transition from special relativity to general relativity.
    - Chapter 25, on the fundamental concepts of general relativity.
- Portions of this chapter are a foundation for the applications of general relativity theory to gravitational waves (Chap. 27) and to cosmology (Chap. 28).

26.1 Overview

Having sketched the fundamentals of Einstein's theory of gravity, general relativity, we shall now illustrate his theory by means of several concrete applications: stars and black holes in this chapter, gravitational waves in Chap. 27, and the large-scale structure and evolution of the universe in Chap. 28.

While stars and black holes are the central thread of this chapter, we study them less for their own intrinsic interest than for their roles as vehicles by which to understand general relativity: Using them we shall elucidate a number of issues that we have already met: the physical and geometric interpretations of spacetime metrics and of coordinate systems, the Newtonian limit of general relativity, the geodesic motion of freely falling particles and photons, local Lorentz frames and the tidal forces measured therein, proper reference frames, the Einstein field equations, the local law of conservation of 4-momentum, and the asymptotic

1

structure of spacetime far from gravitating sources. Stars and black holes will also serve to introduce several new physical phenomena that did not show up in our study of the foundations of general relativity: the gravitational redshift, the "many-fingered" nature of time, event horizons, and spacetime singularities.

We begin this chapter, in Sec. 26.2, by studying the geometry of the curved spacetime outside any static star, as predicted by the Einstein field equation. In Sec. 26.3, we study general relativity's description of the interiors of static stars. In Sec. 26.4, we turn attention to the spherically symmetric gravitational implosion by which a nonrotating star is transformed into a black hole, and to the "Schwarzschild" spacetime geometry outside and inside the resulting static, spherical hole. In Sec. 26.5, we study the "Kerr" spacetime geometry of a spinning black hole. In Sec. 26.6, we elucidate the nature of "time" in the curved spacetimes of general relativity. And in Ex. 26.10, we explore the role of the vacuum Schwarzschild solution of the Einstein field equation as a *wormhole*.

26.2   Schwarzschild's Spacetime Geometry

On January 13, 1916, just seven weeks after formulating the final version of his field equation, $\boldsymbol{G} = 8\pi\boldsymbol{T}$, Albert Einstein read to a meeting of the Prussian Academy of Sciences in Berlin a letter from the eminent German astrophysicist Karl Schwarzschild. Schwarzschild, as a member of the German army, had written from the World-War-One Russian front to tell Einstein of a mathematical discovery he had made: he had found the world's first exact solution to the Einstein field equation.

Written as a line element in a special coordinate system (coordinates named t, r, θ, ϕ) that Schwarzschild invented for the purpose, Schwarzschild's solution takes the form (Schwarzschild 1916a)

$$ds^2 = -(1 - 2M/r)dt^2 + \frac{dr^2}{(1 - 2M/r)} + r^2(d\theta^2 + \sin^2\theta d\phi^2)\,, \qquad (26.1)$$

where M is a constant of integration. The connection coefficients, Riemann tensor, and Ricci and Einstein tensors for this metric can be computed by the methods of Chaps. 23 and 25; see Ex. 26.1. The results are tabulated in Box 26.2. The key bottom line is that the Einstein tensor vanishes. Therefore, the Schwarzschild metric (26.1) is a solution of the Einstein field equations with vanishing stress-energy tensor.

Many readers know already the lore of this subject: The Schwarzschild spacetime is reputed to represent the vacuum exterior of a nonrotating, spherical star; and also the exterior of a spherical star as it implodes to form a black hole; and also the exterior and interior of a nonrotating, spherical black hole; and also a wormhole that connects two different universes or two widely separated regions of our own universe.

How does one discover these physical interpretations of the Schwarzschild metric (26.1)? The tools for discovering them—and, more generally, the tools for interpreting physically any spacetime metric that one encounters—are a central concern of this chapter.

When presented with a line element such as (26.1), one of the first questions one is tempted to ask is "What is the nature of the coordinate system?" Since the metric coefficients

Box 26.2
Connection Coefficients and Curvature Tensors for Schwarzschild

The coordinate basis vectors for the Schwarzschild solution are

$$\vec{e}_t = \frac{\partial}{\partial t}, \ \ \vec{e}_r = \frac{\partial}{\partial r}, \ \ \vec{e}_\theta = \frac{\partial}{\partial \theta}, \ \ \vec{e}_\phi = \frac{\partial}{\partial \phi}; \ \ \vec{e}^{\,t} = \vec{\nabla} t, \ \ \vec{e}^{\,r} = \vec{\nabla} r, \ \ \vec{e}^{\,\theta} = \vec{\nabla} \theta, \ \ \vec{e}^{\,\phi} = \vec{\nabla} \phi. \quad (1)$$

The covariant metric coefficients in this coordinate basis are [cf. Eq. (26.1)]

$$g_{tt} = -\left(1 - \frac{2M}{r}\right) \ , \quad g_{rr} = \frac{1}{(1 - 2M/r)} \ , \quad g_{\theta\theta} = r^2 \ , \quad g_{\phi\phi} = r^2 \sin^2\theta \ ; \quad (2a)$$

and the contravariant metric coefficients are the inverse of these

$$g^{tt} = -\frac{1}{(1 - 2M/r)} \ , \quad g^{rr} = \left(1 - \frac{2M}{r}\right) \ , \quad g^{\theta\theta} = \frac{1}{r^2} \quad g^{\phi\phi} = \frac{1}{r^2 \sin^2\theta} \ . \quad (2b)$$

The nonzero connection coefficients in this coordinate basis are

$$\Gamma^t{}_{rt} = \Gamma^t{}_{tr} = \frac{M}{r^2} \frac{1}{(1 - 2M/r)} \ , \quad \Gamma^r{}_{tt} = \frac{M}{r^2}(1 - 2M/r) \ , \quad \Gamma^r{}_{rr} = -\frac{M}{r^2} \frac{1}{(1 - 2M/r)} \ ,$$

$$\Gamma^r{}_{\theta\theta} = -r(1 - 2M/r) \ , \quad \Gamma^\theta{}_{r\theta} = \Gamma^\theta{}_{\theta r} = \Gamma^\phi{}_{r\phi} = \Gamma^\phi{}_{\phi r} = \frac{1}{r} \ , \quad (3)$$

$$\Gamma^r{}_{\phi\phi} = -r\sin^2\theta(1 - 2M/r) \ , \quad \Gamma^\theta{}_{\phi\phi} = -\sin\theta\cos\theta \ , \quad \Gamma^\phi{}_{\theta\phi} = \Gamma^\phi{}_{\phi\theta} = \cot\theta \ ,$$

The orthonormal basis associated with the above coordinate basis is

$$\vec{e}_{\hat{0}} = \frac{\partial/\partial t}{\sqrt{1 - 2M/r}} \ , \quad \vec{e}_{\hat{r}} = \sqrt{1 - \frac{2M}{r}} \frac{\partial}{\partial r} \ , \quad \vec{e}_{\hat{\theta}} = \frac{1}{r}\frac{\partial}{\partial \theta} \ , \quad \vec{e}_{\hat{\phi}} = \frac{1}{r\sin\theta}\frac{\partial}{\partial \phi} \ . \quad (4)$$

The nonzero connection coefficients in this orthonormal basis are

$$\Gamma^{\hat{r}}{}_{\hat{t}\hat{t}} = \Gamma^{\hat{t}}{}_{\hat{r}\hat{t}} = \frac{M}{r^2\sqrt{1 - 2M/r}} \ , \quad \Gamma^{\hat{\phi}}{}_{\hat{\theta}\hat{\phi}} = -\Gamma^{\hat{\theta}}{}_{\hat{\phi}\hat{\phi}} = \frac{\cot\theta}{r} \ ,$$

$$\Gamma^{\hat{\theta}}{}_{\hat{r}\hat{\theta}} = \Gamma^{\hat{\phi}}{}_{\hat{r}\hat{\phi}} = -\Gamma^{\hat{r}}{}_{\hat{\theta}\hat{\theta}} = -\Gamma^{\hat{r}}{}_{\hat{\phi}\hat{\phi}} = \frac{\sqrt{1 - 2M/r}}{r} \ . \quad (5)$$

The nonzero components of the Riemann tensor in this orthonormal basis are

$$R_{\hat{r}\hat{t}\hat{r}\hat{t}} = -R_{\hat{\theta}\hat{\phi}\hat{\theta}\hat{\phi}} = -\frac{2M}{r^3} \ , \quad R_{\hat{\theta}\hat{t}\hat{\theta}\hat{t}} = R_{\hat{\phi}\hat{t}\hat{\phi}\hat{t}} = -R_{\hat{r}\hat{\phi}\hat{r}\hat{\phi}} = -R_{\hat{r}\hat{\theta}\hat{r}\hat{\theta}} = \frac{M}{r^3} \ , \quad (6)$$

and those obtainable from these via the symmetries (25.42a) of Riemann. The Ricci tensor, curvature scalar, and Einstein tensor all vanish—which implies that the Schwarzschild metric is a solution of the vacuum Einstein field equations.

will be different in some other coordinate system, surely one must know something about the coordinates in order to interpret the line element.

Remarkably, one need not go to the inventor of the coordinates to find out their nature. Instead one can turn to the line element itself: the line element (or metric coefficients) contain full information not only about the details of the spacetime geometry, but also about the nature of the coordinates. The line element (26.1) is a good example:

Look first at the 2-dimensional surfaces in spacetime that have constant values of t and r. We can regard $\{\theta, \phi\}$ as a coordinate system on each such 2-surface. The spacetime line element (26.1) tells us that the geometry of the 2-surface is given in terms of those coordinates by

$$^{(2)}ds^2 = r^2(d\theta^2 + \sin^2\theta d\phi^2) \tag{26.2}$$

(where the prefix $^{(2)}$ refers to the dimensionality of the surface). This is the line element (metric) of an ordinary, everyday 2-dimensional sphere expressed in standard spherical polar coordinates. Thus, we have learned that the *Schwarzschild spacetime is spherically symmetric*, and moreover, *θ and ϕ are standard spherical polar coordinates*. This is an example of extracting from a metric information about both the coordinate-independent spacetime geometry and the coordinate system being used.

Note, further, from Eq. (26.2), that the circumferences and surface areas of the spheres $(t, r) = $ const in Schwarzschild spacetime are given by

$$\boxed{\text{circumference} = 2\pi r , \quad \text{area} = 4\pi r^2} . \tag{26.3}$$

This tells us one aspect of the geometric interpretation of the r coordinate: r is a *radial coordinate* in the sense that the circumferences and surface areas of the spheres in Schwarzschild spacetime are expressed in terms of r in the standard manner (26.3). We must not go further, however, and assert that r is radius in the sense of being the distance from the center of one of the spheres to its surface. The center, and the line from center to surface, do not lie on the sphere itself and they thus are not described by the spherical line element (26.2). Moreover, since we know that spacetime is curved, we have no right to expect that the distance from the center of a sphere to its surface will be given by distance = circumference$/2\pi = r$ as in flat spacetime.

Returning to the Schwarzschild line element (26.1), let us examine several specific regions of spacetime: At "radii" r large compared to the integration constant M, the line element (26.1) takes the form

$$ds^2 = -dt^2 + dr^2 + r^2(d\theta^2 + \sin^2\theta d\phi^2) . \tag{26.4}$$

This is the line element of flat spacetime, $ds^2 = -dt^2 + dx^2 + dy^2 + dz^2$ written in spherical polar coordinates $[x = r\sin\theta\cos\phi,\ y = r\sin\theta\sin\phi,\ z = r\cos\theta]$. Thus, *Schwarzschild spacetime is asymptotically flat in the region of large radii $r/M \to \infty$*. This is just what one might expect physically when one gets far away from all sources of gravity. Thus, it is reasonable to presume that the Schwarzschild spacetime geometry is that of some sort of isolated, gravitating body which is located in the region $r \sim M$.

The large-r line element (26.4) not only reveals that Schwarzschild spacetime is asymptotically flat; it also shows that in the asymptotically flat region the Schwarzschild coordinate

t is the time coordinate of a Lorentz reference frame. Notice that the region of strong space-time curvature has a boundary (say, $r \sim 100M$) that remains forever fixed relative to the asymptotically Lorentz spatial coordinates $x = r\sin\theta\cos\phi$, $y = r\sin\theta\sin\phi$, $z = r\cos\theta$. This means that the asymptotic Lorentz frame can be regarded as the body's *asymptotic rest frame*. We conclude, then, that *far from the body the Schwarzschild t coordinate becomes the Lorentz time of the body's asymptotic rest frame, and the Schwarzschild r, θ, ϕ coordinates become spherical polar coordinates in the body's asymptotic rest frame.*

As we move inward from $r = \infty$, we gradually begin to see spacetime curvature. That curvature shows up, at $r \gg M$, in slight deviations of the Schwarzschild metric coefficients from those of a Lorentz frame: to first order in M/r the line element (26.1) becomes

$$ds^2 = -\left(1 - \frac{2M}{r}\right)dt^2 + \left(1 + \frac{2M}{r}\right)dr^2 + r^2(d\theta^2 + \sin^2\theta d\phi^2) \ . \tag{26.5}$$

or, equivalently, in Cartesian spatial coordinates,

$$ds^2 = -\left(1 - \frac{2M}{\sqrt{x^2 + y^2 + z^2}}\right)dt^2 + dx^2 + dy^2 + dz^2 + \frac{2M}{r}\left(\frac{x}{r}dx + \frac{y}{r}dy + \frac{z}{r}dz\right)^2 \ . \tag{26.6}$$

It is reasonable to expect that, at these large radii where the curvature is weak, Newtonian gravity will be a good approximation to Einsteinian gravity. In Sec. 25.9.1 of the last chapter, we studied in detail the transition from general relativity to Newtonian gravity, and found that, in nearly Newtonian situations, if one uses a nearly globally Lorentz coordinate system (as we are doing), the line element should take the form [Eq. (25.74)]

$$ds^2 = -(1 + 2\Phi)dt^2 + (\delta_{jk} + h_{jk})dx^j dx^k + 2h_{tj}dt\,dx^j \ , \tag{26.7}$$

where $h_{\mu\nu}$ are metric corrections that are very small compared to unity, and where Φ (which shows up in the time-time part of the metric) is the Newtonian potential. Direct comparison of (26.7) with (26.6) shows that a Newtonian description of the body's distant gravitational field will entail a Newtonian potential given by

$$\Phi = -\frac{M}{r} \tag{26.8}$$

($\Phi = -GM/r$ in cgs units). This, of course, is the external Newtonian field of a body with mass M. Thus, *the integration constant M in the Schwarzschild line element is the mass which characterizes the body's distant, nearly Newtonian gravitational field.* This is an example of reading the mass of a body off the asymptotic form of the metric (Sec. 25.9.3).

Notice that the asymptotic metric here [Eq. (26.5)] differs in its spatial part from that in Sec. 25.9.3 [Eq. (25.89d)]. This difference arises from the use of different radial coordinates here and there: If we define $\bar{r}$ by $r = \bar{r} + M$ at radii $r \gg M$, then to linear order in M/r, the asymptotic Schwarzschild metric (26.5) becomes

$$ds^2 = -\left(1 - \frac{2M}{\bar{r}}\right)dt^2 + \left(1 + \frac{2M}{\bar{r}}\right)[d\bar{r}^2 + \bar{r}^2(d\theta^2 + \sin^2\theta d\phi^2)] \ , \tag{26.9}$$

which is the same as Eq. (25.89d) with vanishing angular momentum $S_j = 0$. This easy change of the spatial part of the metric reinforces the fact that one reads the asymptotic Newtonian potential and the source's mass M off the *time-time* components of the metric, and not the spatial part of the metric.

We can describe, in operational terms, the physical interpretation of M as the body's mass as follows: Suppose that a test particle (e.g., a small planet) moves around our central body in a circular orbit with radius $r \gg M$. A Newtonian analysis of the orbit predicts that, as measured using Newtonian time, the period of the orbit will be $P = 2\pi(r^3/M)^{\frac{1}{2}}$ (one of Kepler's laws). Moreover, since Newtonian time is very nearly equal to the time t of the nearly Lorentz coordinates used in Eq. (26.5) (cf. Sec. 25.9.1), and since that t is Lorentz time in the body's relativistic, asymptotic rest frame, the orbital period as measured by observers at rest in the asymptotic rest frame must be $P = 2\pi(r^3/M)^{\frac{1}{2}}$. Thus, *M is the mass that appears in Kepler's laws for the orbits of test particles far from the central body*. This quantity is often called the body's "active gravitational mass," since it is the mass that characterizes the body's gravitational pull. It is also called the body's "total mass-energy" because it turns out to include all forms of mass and energy that the body possesses (rest mass, internal kinetic energy, and all forms of internal binding energy including gravitational).

We note, in passing, that one can use general relativity to deduce the Keplerian role of M without invoking the Newtonian limit: We place a test particle in the body's equatorial plane $\theta = \pi/2$ at a radius $r \gg M$, and we give it an initial velocity that lies in the equatorial plane. Then symmetry guarantees the body will remain in the equatorial plane: there is no way to prefer going toward north, $\theta < \pi/2$, or toward south, $\theta > \pi/2$. We, further, adjust the initial velocity so the particle remains always at a fixed radius. Then the only nonvanishing components $u^\alpha = dx^\alpha/d\tau$ of the particle's 4-velocity will be $u^t = dt/d\tau$ and $u^\phi = d\phi/d\tau$. The particle's orbit will be governed by the geodesic equation $\nabla_{\vec{u}} \vec{u} = 0$, where $\vec{u}$ is its 4-velocity. The radial component of this geodesic equation, computed in Schwarzschild coordinates, is [cf. Eq. (25.14b) with a switch from affine parameter ζ to proper time $\tau = m\zeta$]

$$\frac{d^2r}{d\tau^2} = -\Gamma^r{}_{\mu\nu}\frac{dx^\mu}{d\tau}\frac{dx^\nu}{d\tau} = -\Gamma^r{}_{tt}\frac{dt}{d\tau}\frac{dt}{d\tau} - \Gamma^r{}_{\phi\phi}\frac{d\phi}{d\tau}\frac{d\phi}{d\tau} \ . \tag{26.10}$$

(Here we have used the vanishing of all $dx^\alpha/d\tau$ except the t and ϕ components, and have used the vanishing of $\Gamma^r{}_{t\phi} = \Gamma^r{}_{\phi t}$ [Eq. (3) of Box 26.2].) Since the orbit is circular, with fixed r, the left side of Eq. (26.10) must vanish; and correspondingly the right side gives

$$\frac{d\phi}{dt} = \frac{d\phi/d\tau}{dt/d\tau} = \left(-\frac{\Gamma^r{}_{tt}}{\Gamma^r{}_{\phi\phi}}\right)^{\frac{1}{2}} = \left(\frac{M}{r^3}\right)^{\frac{1}{2}} \ , \tag{26.11}$$

where we have used the values of the connection coefficients from Eq. (3) of Box 26.2, specialized to the equatorial plane $\theta = \pi/2$. Equation (26.11) tells us that the amount of coordinate time t required for the particle to circle the central body once, $0 \le \phi \le 2\pi$, is $\Delta t = 2\pi(r^3/M)^{\frac{1}{2}}$. Since t is the Lorentz time of the body's asymptotic rest frame, this means that observers in the asymptotic rest frame will measure for the particle an orbital period $P = \Delta t = 2\pi(r^3/M)^{\frac{1}{2}}$. This, of course, is the same result as we obtained from the Newtonian limit—but our relativistic analysis shows it to be true for circular orbits of arbitrary radius r, not just for $r \gg M$.

Next we shall move inward, from the asymptotically flat region of Schwarzschild space-time, toward smaller and smaller radii. As we do so, the spacetime geometry becomes more and more strongly curved, and the Schwarzschild coordinate system becomes less and less Lorentz. As an indication of extreme deviations from Lorentz, notice that the signs of the metric coefficients

$$\frac{\partial}{\partial t} \cdot \frac{\partial}{\partial t} = g_{tt} = -\left(1 - \frac{2M}{r}\right) \ , \quad \frac{\partial}{\partial r} \cdot \frac{\partial}{\partial r} = g_{rr} = \frac{1}{(1 - 2M/r)} \tag{26.12}$$

get reversed as one moves from $r > 2M$ through $r = 2M$ and into the region $r < 2M$. Correspondingly, outside $r = 2M$, world lines of changing t but constant r, θ, ϕ are timelike, while inside $r = 2M$, those world lines are spacelike; and similarly outside $r = 2M$ world lines of changing r but constant t, θ, ϕ are spacelike, while inside they are timelike. In this sense, *outside $r = 2M$, t plays the role of a time coordinate and r the role of a space coordinate; while inside $r = 2M$, t plays the role of a space coordinate and r the role of a time coordinate.* Moreover, this role reversal occurs without any change in the role of r as $1/2\pi$ times the circumference of circles around the center [Eq. (26.3)].

Historically, for many decades this role reversal presented severe conceptual problems, even to the best experts in general relativity. We shall return to it in Sec. 26.4 below. Henceforth we shall refer to the location of role reversal, $r = 2M$, as the *gravitational radius* of the Schwarzschild spacetime. Throughout the rest of this section and all of Sec. 26.3, we shall confine attention to the region $r > 2M$, outside the gravitational radius. In Sec. 26.4 we shall seek a clear understanding of the "interior" region, $r < 2M$.

Notice that the metric coefficients in the Schwarzschild line element (26.1) are all independent of the coordinate t. This means that the geometry of spacetime itself is invariant under the translation $t \to t +$ constant. At radii $r > 2M$, where t plays the role of a time coordinate, $t \to t +$ constant is a time translation; and, correspondingly, *the Schwarzschild spacetime geometry is time-translation-invariant, i.e., "static," outside the gravitational radius.*

****

EXERCISES

Exercise 26.1 *Practice: Connection Coefficients and Riemann tensor in the Schwarzschild Metric*

(a) Explain why, for the Schwarzschild metric (26.1), the metric coefficients in the coordinate basis have the values given in Eqs. (2a,b) of Box 26.2.

(b) Using tensor-analysis software on a computer,[1] derive the connection coefficients given in Eq. (3) of Box 26.2.

(c) Show that the basis vectors in Eqs. (4) of Box 26.2 are orthonormal.

---

[1]e.g., the simple Mathematica program in Appendix C of Hartle (2003), which is available on that book's website, `http://web.physics.ucsb.edu/~gravitybook/` .

(d) Using tensor-analysis software on a computer, derive the connection coefficients (5) and Riemann components (6) of Box 26.2 in the orthonormal basis.

Exercise 26.2 *Example: The Bertotti-Robinson solution of the Einstein field equation*
Bruno Bertotti (1959) and Ivor Robinson (1959) have independently solved the Einstein field equation to obtain the following metric for a universe endowed with a uniform magnetic field:

$$ds^2 = Q^2(-dt^2 + \sin^2 t dz^2 + d\theta^2 + \sin^2 \theta d\phi^2) . \tag{26.13}$$

Here

$$Q = \text{const} , \quad 0 \le t \le \pi , \quad -\infty < z < +\infty , \quad 0 \le \theta \le \pi , \quad 0 \le \phi \le 2\pi . \tag{26.14}$$

If one computes the Einstein tensor from the metric coefficients of the line element (26.13) and equates it to 8π times a stress-energy tensor, one finds a stress-energy tensor which is precisely that of an electromagnetic field [Eqs. (2.76) and (2.81)] lifted, unchanged, into general relativity. The electromagnetic field is one which, as measured in the local Lorentz frame of an observer with fixed z, θ, ϕ (a "static" observer), has vanishing electric field and has a magnetic field with magnitude independent of where the observer is located in spacetime and with direction along $\partial/\partial z$. In this sense, the spacetime (26.13) is that of a homogeneous magnetic universe. Discuss the geometry of this universe and the nature of the coordinates t, z, θ, ϕ. More specifically:

(a) Which coordinate increases in a timelike direction and which coordinates in spacelike directions?

(b) Is this universe spherically symmetric?

(c) Is this universe cylindrically symmetric?

(d) Is this universe asymptotically flat?

(e) How does the geometry of this universe change as t ranges from 0 to π. [Hint: show that the curves $\{(z, \theta, \phi) = \text{const}, t = \tau/Q\}$ are timelike geodesics—the world lines of the static observers referred to above. Then argue from symmetry, or use the result of Ex. 25.4.]

(f) Give as complete a characterization as you can of the coordinates t, z, θ, ϕ.

$$**************************$$

26.3 Static Stars

26.3.1 Birkhoff's Theorem

In 1923, George Birkhoff, a professor of mathematics at Harvard, proved a remarkable theorem:[2] *The Schwarzschild spacetime geometry is the unique spherically symmetric solution*

---

[2]For a textbook proof see Sec. 32.2 of MTW.

of the vacuum Einstein field equation $\boldsymbol{G} = 0$. This Birkhoff theorem can be restated in more operational terms as follows: Suppose that you find a solution of the vacuum Einstein field equation, written as a set of metric coefficients $g_{\bar{\alpha}\bar{\beta}}$ in some coordinate system $\{x^{\bar{\mu}}\}$. Suppose, further, that these $g_{\bar{\alpha}\bar{\beta}}(x^{\bar{\mu}})$ exhibit spherical symmetry, but do not coincide with the Schwarzschild expressions [Eqs. (2a) of Box 26.2]. Then Birkhoff guarantees the existence of a coordinate transformation from your coordinates $x^{\bar{\mu}}$ to Schwarzschild's coordinates x^{ν} such that, when that transformation is performed, the resulting new metric components $g_{\alpha\beta}(x^{\nu})$ have precisely the Schwarzschild form [Eq. (2a) of Box 26.2]. For an example, see Ex. 26.3. This implies that, thought of as a coordinate-independent spacetime geometry, the Schwarzschild solution is completely unique.

Consider, now, a static, spherically symmetric star (e.g. the sun) residing alone in an otherwise empty universe (or, more realistically, residing in our own universe but so far from all other gravitating matter that we can ignore all other sources of gravity when studying it). Since the star's interior is spherical, it is reasonable to presume that the exterior will be spherical; and since the exterior is also vacuum ($\boldsymbol{T} = 0$), its spacetime geometry must be that of Schwarzschild. If the circumference of the star's surface is $2\pi R$ and its surface area is $4\pi R^2$, then that surface must reside at the location $r = R$ in the Schwarzschild coordinates of the exterior. In other words, the spacetime geometry will be described by the Schwarzschild line element (26.1) at radii $r > R$, but by something else inside the star, at $r < R$.

Since real atoms with finite rest masses reside on the star's surface, and since such atoms move along timelike world lines, it must be that the world lines $\{r = R, \theta = \text{const}, \phi = \text{const}, t \text{ varying}\}$ are timelike. From the Schwarzschild invariant interval (26.1) we read off the squared proper time $d\tau^2 = -ds^2 = (1 - 2M/R)dt^2$ along those world lines. This $d\tau^2$ is positive (timelike world line) if and only if $R > 2M$. Thus, *a static star with total mass-energy (active gravitational mass) M can never have a circumference smaller than $2\pi R = 4\pi M$.* Restated in conventional units:

$$\boxed{\frac{\text{circumference}}{2\pi} = R \equiv \begin{pmatrix}\text{Radius} \\ \text{of star}\end{pmatrix} > 2M = \frac{2GM}{c^2} = 2.953\,\text{km}\left(\frac{M}{M_\odot}\right) \equiv \begin{pmatrix}\text{gravitational} \\ \text{radius}\end{pmatrix}}$$

(26.15)

Here $M_\odot$ is the mass of the sun. The sun satisfies this constraint by a huge margin: $R = 7\times10^5$km. A one-solar-mass white-dwarf star satisfies it by a smaller margin: $R \simeq 6\times10^3$km. And a one-solar-mass neutron star satisfies it by only a modest margin: $R \simeq 10$km. For a pedagogical and detailed discussion see, e.g., Shapiro and Teukolsky (1983).

****

EXERCISES

Exercise 26.3 *Example: Schwarzschild Geometry in Isotropic Coordinates*

(a) It turns out that the following line element is a solution of the vacuum Einstein field equation $\boldsymbol{G} = 0$:

$$\boxed{ds^2 = -\left(\frac{1 - M/2\bar{r}}{1 + M/2\bar{r}}\right)^2 dt^2 + \left(1 + \frac{M}{2\bar{r}}\right)^4 [d\bar{r}^2 + \bar{r}^2(d\theta^2 + \sin^2\theta d\phi^2)]}.$$

(26.16)

Since this solution is spherically symmetric, Birkhoff's theorem guarantees it must represent the standard Schwarzschild spacetime geometry in a coordinate system that differs from Schwarzschild's. Show that this is so by exhibiting a coordinate transformation that converts this line element into (26.1). Note: the t, $\bar{r}$, θ, ϕ coordinates are called *isotropic* because in them the spatial part of the line element is a function of $\bar{r}$ times the 3-dimensional Euclidean line element, and Euclidean geometry picks out at each point in space no preferred spatial directions, i.e., it is isotropic.

(b) Show that at large radii $r \gg M$, the line element (26.16) takes the form (25.89c) discussed in Chap. 25, but with vanishing spin angular momentum $\mathbf{S} = 0$.

Exercise 26.4 *Example: Gravitational Redshift of Light From a Star's Surface*
Consider a photon emitted by an atom at rest on the surface of a static star with mass M and radius R. Analyze the photon's motion in the Schwarzschild coordinate system of the star's exterior, $r \geq R > 2M$; and, in particular, compute the "gravitational redshift" of the photon by the following steps:

(a) Since the emitting atom is very nearly an "ideal clock," it gives the emitted photon very nearly the same frequency ν_{em}, as measured in the atom's proper reference frame, as it would give were it in an earth laboratory or floating in free space. Thus, the proper reference frame of the emitting atom is central to a discussion of the photon's properties and behavior. Show that the basis vectors of that proper reference frame are

$$\vec{e}_{\hat{0}} = \frac{1}{\sqrt{1 - 2M/r}}\frac{\partial}{\partial t} \,, \quad \vec{e}_{\hat{r}} = \sqrt{1 - 2M/r}\frac{\partial}{\partial r} \,, \quad \vec{e}_{\hat{\theta}} = \frac{1}{r}\frac{\partial}{\partial \theta} \,, \quad \vec{e}_{\hat{\phi}} = \frac{1}{r \sin \theta}\frac{\partial}{\partial \phi} \,, \quad (26.17)$$

with $r = R$ (the star's radius). As part of your proof, show that these basis vectors are orthonormal.

(b) Explain why $h\nu_{\mathrm{em}} = -p_{\hat{0}} = -\vec{p} \cdot \vec{e}_{\hat{0}}$ at the moment of photon emission. (Here and below h is Planck's constant and $\vec{p}$ is the photon's 4-momentum.)

(c) Show that the covariant time-component of the photon 4-momentum in the Schwarzschild coordinate basis is $p_t = -\sqrt{1 - 2M/R}\, h\nu_{\mathrm{em}}$ at the moment of emission.

(d) Show that as the photon flies out (radially or nonradially) toward $r = \infty$, the coordinate-time component of its 4-momentum, p_t, is conserved. [*Hint*: recall the result of Ex. 25.4a.]

(e) Show that, when received by an observer at rest relative to the star and very far away from it, the photon is measured by that observer to have frequency $\nu_{\mathrm{rec}} = -p_t/h$.

(f) Show that the photon is redshifted by an amount

$$\boxed{\frac{\lambda_{\mathrm{rec}} - \lambda_{\mathrm{em}}}{\lambda_{\mathrm{em}}} = \frac{1}{\sqrt{1 - 2M/R}} - 1} \,, \quad (26.18)$$

where $\lambda_{\rm rec}$ is the wavelength that the photon's spectral line exhibits at the receiver and $\lambda_{\rm em}$ is the wavelength that the emitting kind of atom would produce in an earth laboratory. Note that for a nearly Newtonian star, i.e. one with $R \gg M$, this redshift becomes $\simeq M/R = GM/Rc^2$.

(g) Evaluate this redshift for the earth, for the sun, and for a 1.4-solar-mass, 10-kilometer-radius neutron star.

<center>***************************</center>

26.3.2 Stellar Interior

We shall now take a temporary detour away from our study of the Schwarzschild geometry in order to discuss the interior of a static, spherical star. We do so less because of an interest in stars than because the detour will illustrate the process of solving the Einstein field equation and the role of the contracted Bianchi identity in the solution process.

Since the star's spacetime geometry is to be static and spherically symmetric, we can introduce as coordinates in its interior: (i) spherical polar angular coordinates θ and ϕ, (ii) a radial coordinate r such that the circumferences of the spheres are $2\pi r$, and (iii) a time coordinate $\bar{t}$ such that the metric coefficients are independent of $\bar{t}$. By their geometrical definitions, these coordinates will produce a spacetime line element of the form

$$ds^2 = g_{\bar{t}\bar{t}}d\bar{t}^2 + 2g_{\bar{t}r}d\bar{t}dr + g_{rr}dr^2 + r^2(d\theta^2 + \sin^2\theta d\phi^2) , \qquad (26.19)$$

with $g_{\alpha\beta}$ independent of $\bar{t}$, θ, and ϕ. Metric coefficients $g_{\bar{t}\theta}$, $g_{r\theta}$, $g_{\bar{t}\phi}$, $g_{r\phi}$ are absent from (26.19) because they would break the spherical symmetry: they would distinguish the $+\phi$ direction from $-\phi$ or $+\theta$ from $-\theta$ since they would give nonzero values for the scalar products of $\partial/\partial\phi$ or $\partial/\partial\theta$ with $\partial/\partial t$ or $\partial/\partial r$. [Recall: the metric coefficients in a coordinate basis are $g_{\alpha\beta} = \boldsymbol{g}(\partial/\partial x^\alpha, \partial/\partial x^\beta) = (\partial/\partial x^\alpha)\cdot(\partial/\partial x^\beta)$.] We can get rid of the off-diagonal $g_{\bar{t}r}$ term in the line element (26.19) by specializing the time coordinate: The coordinate transformation

$$\bar{t} = t - \int \left(\frac{g_{\bar{t}r}}{g_{\bar{t}\bar{t}}}\right) dr . \qquad (26.20)$$

brings the line element into the form

$$\boxed{ds^2 = -e^{2\Phi}dt^2 + e^{2\Lambda}dr^2 + r^2(d\theta^2 + \sin^2\theta d\phi^2)} . \qquad (26.21)$$

Here we have introduced the names $e^{2\Phi}$ and $e^{2\Lambda}$ for the time-time and radial-radial metric coefficients. The signs of these coefficients (negative for g_{tt} and positive for g_{rr}) are dictated by the fact that inside the star, as on its surface, real atoms move along world lines of constant r, θ, ϕ and changing t, and thus those world lines must be timelike. The name $e^{2\Phi}$ ties in with the fact that, when gravity is nearly Newtonian, the time-time metric coefficient $-e^{2\Phi}$ must reduce to $-(1+2\Phi)$, with Φ the Newtonian potential [Eq. (25.74)]. Thus, the Φ

used in (26.21) is a generalization of the Newtonian potential to relativistic, spherical, static gravitational situations.

In order to solve the Einstein field equation for the star's interior, we must specify the stress-energy tensor. Stellar material is excellently approximated by a perfect fluid; and since our star is static, at any point inside the star the fluid's rest frame has constant r, θ, ϕ. Correspondingly, the 4-velocity of the fluid is

$$\boxed{\vec{u} = e^{-\Phi}\frac{\partial}{\partial t}}\ . \tag{26.22}$$

Here the factor $e^{-\Phi}$ guarantees that the 4-velocity will have unit length, as it must.

This fluid, of course, is not freely falling. Rather, in order for a fluid element to remain always at fixed r, θ, ϕ, it must accelerate relative to local freely falling observers with a 4-acceleration $\vec{a} \equiv \nabla_{\vec{u}}\vec{u} \neq 0$; i.e., $a^{\alpha} = u^{\alpha}{}_{;\mu}u^{\mu} \neq 0$. Symmetry tells us that this 4-acceleration cannot have any θ or ϕ components; and orthogonality of the 4-acceleration to the 4-velocity tells us that it cannot have any t component. The r component, computed from $a^{r} = u^{r}{}_{;\mu}u^{\mu} = \Gamma^{r}{}_{00}u^{0}u^{0}$, is $a^{r} = e^{-2\Lambda}\Phi_{,r}$; and thus,

$$\boxed{\vec{a} = e^{-2\Lambda}\ \Phi_{,r}\frac{\partial}{\partial r}}\ . \tag{26.23}$$

Each fluid element can be thought of as carrying with itself an orthonormal set of basis vectors

$$\boxed{\vec{e}_{\hat{0}} = \vec{u} = e^{-\Phi}\frac{\partial}{\partial t}\ ,\quad \vec{e}_{\hat{r}} = e^{-\Lambda}\frac{\partial}{\partial r}\ ,\quad \vec{e}_{\hat{\theta}} = \frac{1}{r}\frac{\partial}{\partial\theta}\ ,\quad \vec{e}_{\hat{\phi}} = \frac{1}{r\sin\theta}\frac{\partial}{\partial\phi}}\ ; \tag{26.24a}$$

$$\boxed{\vec{e}^{\hat{0}} = e^{\Phi}\vec{\nabla}t\ ,\quad \vec{e}^{\hat{r}} = e^{\Lambda}\vec{\nabla}r\ ,\quad \vec{e}^{\hat{\theta}} = r\vec{\nabla}\theta\ ,\quad \vec{e}^{\hat{\phi}} = r\sin\theta\vec{\nabla}\phi}\ . \tag{26.24b}$$

These basis vectors play two independent roles: (i) One can regard the tangent space of each event in spacetime as being spanned by the basis (26.24), specialized to that event. From this viewpoint, (26.24) constitutes an orthonormal, non-coordinate basis that covers every tangent space of the star's spacetime. This basis is called the fluid's *orthonormal, local-rest-frame basis*. (ii) One can focus attention on a specific fluid element, which moves along the world line $r = r_o$, $\theta = \theta_o$, $\phi = \phi_o$; and one can construct the proper reference frame of that fluid element in the same manner as we constructed the proper reference frame of an accelerated observer in flat spacetime in Sec. 23.5. That proper reference frame is a coordinate system $\{x^{\hat{\alpha}}\}$ whose basis vectors on the fluid element's world line are equal to the basis vectors (26.24):

$$\frac{\partial}{\partial x^{\hat{\mu}}} = \vec{e}_{\hat{\mu}}\ ,\quad \vec{\nabla}x^{\hat{\mu}} = \vec{e}^{\hat{\mu}}\ \text{ at } x^{\hat{j}} = 0\ . \tag{26.25a}$$

More specifically: the proper-reference-frame coordinates $x^{\hat{\mu}}$ are given, to second-order in spatial distance from the fluid element's world line, by

$$x^{\hat{0}} = e^{\Phi_o}t\ ,\quad x^{\hat{1}} = \int_{r_o}^{r}e^{\Lambda}dr - \frac{1}{2}e^{-\Lambda_o}r_o[(\theta - \theta_o)^2 + \sin^2\theta_o(\phi - \phi_o)^2]\ ,$$

$$x^{\hat{2}} = r(\theta - \theta_o) - \frac{1}{2}r_o\sin\theta_o\cos\theta_o(\phi - \phi_o)^2\ ,\quad x^{\hat{3}} = r\sin\theta(\phi - \phi_o)\ , \tag{26.25b}$$

from which one can verify relation (26.25a) with $\vec{e}_{\hat{\mu}}$ and $\vec{e}^{\hat{\mu}}$ given by (26.24). [In Eqs. (26.25b) and throughout this discussion all quantities with subscripts $_o$ are evaluated on the fluid's world line.] In terms of the proper-reference-frame coordinates (26.25b), the line element (26.21) takes the following form, accurate to first order in distance from the fluid element's world line:

$$ds^2 = -[1 + 2\Phi_{,r}(r - r_o)](dx^{\hat{o}})^2 + \delta_{ij}dx^{\hat{i}}\,dx^{\hat{j}}\ . \tag{26.25c}$$

Notice that the quantity $\Phi_{,r}(r - r_o)$ is equal to the scalar product of (i) the spatial separation $\hat{\mathbf{x}} \equiv (r - r_o)\partial/\partial r + (\theta - \theta_o)\partial/\partial\theta + (\phi - \phi_o)\partial/\partial\phi$ of the "field point" (r, θ, ϕ) from the fluid element's world line, with (ii) the fluid's 4-acceleration (26.23), viewed as a spatial 3-vector $\mathbf{a} = e^{-2\Lambda_o}\Phi_{,r}\partial/\partial r$. Correspondingly, the spacetime line element (26.25c) in the fluid element's proper reference frame takes the standard proper-reference-frame form (23.60b)

$$ds^2 = -(1 + 2\mathbf{a}\cdot\hat{\mathbf{x}})(dx^{\hat{0}})^2 + \delta_{jk}dx^{\hat{j}}\,dx^{\hat{k}}\ , \tag{26.26}$$

accurate to first-order in distance from the fluid element's world line. At second order, as was discussed at the end of Sec. 25.3, there are corrections proportional to the spacetime curvature.

In the local rest frame of the fluid, i.e., when expanded on the fluid's orthonormal rest-frame basis vectors (26.24) or equally well (26.25a), the components $T^{\hat{\alpha}\hat{\beta}} = (\rho + P)u^{\hat{\alpha}}u^{\hat{\beta}} + Pg^{\hat{\alpha}\hat{\beta}}$ of the fluid's stress-energy tensor take on the standard form [Eq. (23.50)]

$$\boxed{T^{\hat{0}\hat{0}} = \rho\ ,\quad T^{\hat{r}\hat{r}} = T^{\hat{\theta}\hat{\theta}} = T^{\hat{\phi}\hat{\phi}} = P}\ , \tag{26.27}$$

corresponding to a rest-frame mass-energy density ρ and isotropic pressure P. By contrast with the simplicity of these local-rest-frame components, the contravariant components $T^{\alpha\beta} = (\rho + P)u^{\alpha}u^{\beta} + Pg^{\alpha\beta}$ in the (t, r, θ, ϕ) coordinate basis are rather more complicated:

$$T^{tt} = e^{-2\Phi}\rho\ ,\quad T^{rr} = e^{-2\Lambda}P\ ,\quad T^{\theta\theta} = r^{-2}P\ ,\quad T^{\phi\phi} = (r\sin\theta)^{-2}P\ . \tag{26.28}$$

This shows one advantage of using orthonormal bases: The components of vectors and tensors are generally simpler in an orthonormal basis than in a coordinate basis. A second advantage occurs when one seeks the physical interpretation of formulae. Because every orthonormal basis is the proper-reference-frame basis of some local observer (the observer with 4-velocity $\vec{u} = \vec{e}_{\hat{o}}$), components measured in such a basis have an immediate physical interpretation in terms of measurements by that observer. For example, $T^{\hat{0}\hat{0}}$ is the total density of mass-energy measured by the local observer. By contrast, components in a coordinate basis typically do not have a simple physical interpretation.

26.3.3 Local Conservation of Energy and Momentum

Before inserting the perfect-fluid stress-energy tensor (26.27) into the Einstein field equation, we shall impose on it the local law of conservation of 4-momentum, $\vec{\nabla}\cdot\boldsymbol{T} = 0$. In doing so we shall require from the outset that, since the star is to be static and spherical, its density ρ and pressure P must be independent of t, θ, and ϕ; i.e., like the metric coefficients Φ and Λ, they must be functions of radius r only.

The most straightforward way to impose 4-momentum conservation is to equate to zero the quantities

$$T^{\alpha\beta}{}_{;\beta} = \frac{\partial T^{\alpha\beta}}{\partial x^{\beta}} + \Gamma^{\beta}{}_{\mu\beta}T^{\alpha\mu} + \Gamma^{\alpha}{}_{\mu\beta}T^{\mu\beta} = 0 \tag{26.29}$$

in our coordinate basis, making use of expressions (26.28) for the contravariant components of the stress-energy tensor, and the connection coefficients and metric components given in Box 26.2.

This straightforward calculation requires a lot of work. Much better is an analysis based on the local proper reference frame of the fluid:

The temporal component of $\vec{\nabla}\cdot\boldsymbol{T} = 0$ in that reference frame, i.e. the projection $\vec{u}\cdot(\vec{\nabla}\cdot\boldsymbol{T}) = 0$ of this conservation law onto the time basis vector $\vec{e}_{\hat{0}} = e^{-\Phi}\partial/\partial t = \vec{u}$, represents energy conservation as seen by the fluid—the first law of thermodynamics:

$$\frac{d(\rho V)}{d\tau} = -P\frac{dV}{d\tau} \ . \tag{26.30}$$

Here τ is proper time as measured by the fluid elment we are following and V is the fluid element's volume. (This equation is derived in Ex. 2.26b, in a special relativistic context; but since it involves only one derivative, there is no danger of curvature coupling, so that derivation and the result can be lifted without change into general relativity, i.e. into the star's curved spacetime; cf. Ex. 26.5a.) Now, inside this static star, the fluid element sees and feels no changes. Its density ρ, pressure P and volume V remain always constant along the fluid element's world line, and energy conservation is therefore guaranteed to be satisfied already. Equation (26.30) tells us nothing new.

The spatial part of $\vec{\nabla}\cdot\boldsymbol{T} = 0$ in the fluid's local rest frame can be written in geometric form as $\boldsymbol{P}\cdot(\vec{\nabla}\cdot\boldsymbol{T}) = 0$. Here $\boldsymbol{P} \equiv \boldsymbol{g} + \vec{u}\otimes\vec{u}$ is the tensor that projects all vectors into the 3-surface orthogonal to $\vec{u}$, i.e. into the fluid's local 3-surface of simultaneity (Exs. 2.10 and 25.1b). By inserting the perfect-fluid stress-energy tensor $\boldsymbol{T} = (\rho + P)\vec{u}\otimes\vec{u} + P\boldsymbol{g} = \rho\vec{u}\otimes\vec{u} + P\boldsymbol{P}$ into $\boldsymbol{P}\cdot(\vec{\nabla}\cdot\boldsymbol{T}) = 0$, reexpressing the result in slot-naming index notation, and carrying out some index gymnastics, we must obtain the same result as in special relativity (Ex. 2.26c):

$$(\rho + P)\vec{a} = -\boldsymbol{P}\cdot\vec{\nabla}P \tag{26.31}$$

(cf. Ex. 26.5). Here $\vec{a}$ is the fluid's 4-velocity. Recall from Ex. 2.27 that for a perfect fluid $\rho + P$ is the inertial mass per unit volume. Therefore, Eq. (26.31) says that *the fluid's inertial mass per unit volume times its 4-acceleration is equal to the negative of its pressure gradient, projected orthogonal to its 4-velocity.* Since both sides of Eq. (26.31) are purely spatially directed as seen in the fluid's local proper reference frame, we can rewrite this equation in 3-dimensional language as

$$\boxed{(\rho + P)\mathbf{a} = -\boldsymbol{\nabla}P} \ . \tag{26.32}$$

A Newtonian physicist, in the proper reference frame, would identify $-\mathbf{a}$ as the local gravitational acceleration, $\boldsymbol{g}$ [cf. Eq. (23.68)], and correspondingly would rewrite Eq. (26.31) as

$$\boldsymbol{\nabla}P = (\rho + P)\boldsymbol{g} \ . \tag{26.33}$$

This is the standard equation of hydrostatic equilibrium for a fluid in an earth-bound laboratory (or swimming pool or lake or ocean), except for the presence of the pressure P in the inertial mass per unit volume. On earth the typical pressures of fluids, even deep in the ocean, are only $P \lesssim 10^9$ dyne/cm$^2 \simeq 10^{-12}$ g/cm$^3 \lesssim 10^{-12}\rho$; and thus, to extremely good accuracy one can ignore the contribution of pressure to the inertial mass density. However, deep inside a neutron star, P may be within a factor 2 of ρ, so the contribution of P cannot be ignored.

We can convert the law of force balance (26.31) into an ordinary differential equation for the pressure P by evaluating its components in the fluid's proper reference frame. The 4-acceleration (26.23) is purely radial; its radial component is $a^{\hat{r}} = e^{-\Lambda}\Phi_{,r} = \Phi_{,\hat{r}}$. The gradient of the pressure is also purely radial and its radial component is $P_{;\hat{r}} = P_{,\hat{r}} = e^{-\Lambda}P_{,r}$. Therefore, the law of force balance reduces to

$$\frac{dP}{dr} = -(\rho + P)\frac{d\Phi}{dr} \ . \tag{26.34}$$

****

EXERCISES

Exercise 26.5 *Practice and Derivation: Local Conservation of Energy and Momentum for Perfect Fluid*

(a) Use index manipulations to show that in general (not just inside a static star), for a perfect fluid with $T^{\alpha\beta} = (\rho+P)u^\alpha u^\beta + Pg^{\alpha\beta}$, the law of energy conservation $u_\alpha T^{\alpha\beta}{}_{;\beta} = 0$ reduces to the first law of thermodynamics (26.30). [Hint: you will need the relation $u^\mu{}_{;\mu} = (1/V)(dV/d\tau)$; cf. Ex. 2.24.]

(b) Similarly show that $P_{\mu\alpha}T^{\alpha\beta}{}_{;\beta} = 0$ reduces to the force-balance law (26.31).

****

26.3.4 Einstein Field Equation

Turn, now, to the Einstein field equation. In order to impose it, we must first compute in our $\{t, r, \theta, \phi\}$ coordinate system the components of the Einstein tensor $G_{\alpha\beta}$. In general, the Einstein tensor has 10 independent components. However, the symmetries of the line element (26.21) impose identical symmetries on the Einstein tensor computed from it: The only nonzero components in the fluid's proper reference frame will be $G^{\hat{0}\hat{0}}$, $G^{\hat{r}\hat{r}}$, and $G^{\hat{\theta}\hat{\theta}} = G^{\hat{\phi}\hat{\phi}}$; and these three independent components will be functions of radius r only. Correspondingly, the Einstein equation will produce three independent differential equations for our four unknowns: the metric coefficients ("gravitational potentials") Φ and Λ [Eq. (26.21)], and the radial distribution of density ρ and pressure P.

These three independent components of the Einstein equation will actually be redundant with the law of hydrostatic equilibrium (26.34). One can see this as follows: If we had not yet imposed the law of 4-momentum conservation, then the Einstein equation $\boldsymbol{G} = 8\pi\boldsymbol{T}$, together with the Bianchi identity $\vec{\nabla} \cdot \boldsymbol{G} \equiv 0$ [Eq. (25.64)], would enforce $\vec{\nabla} \cdot \boldsymbol{T} = 0$. More explicitly, our three independent components of the Einstein equation together would imply the law of radial force balance, i.e., of hydrostatic equilibrium (26.34). Since we have already imposed (26.34), we need evaluate only two of the three independent components of the Einstein equation; they will give us full information.

A long and rather tedious calculation (best done on a computer), based on the metric coefficients of (26.21) and on Eqs. (23.38), (25.47), (25.43), (25.46), and (25.63) produces for the time-time and radial-radial components of the Einstein tensor, and thence of the Einstein field equation,

$$G^{\hat{0}\hat{0}} = -\frac{1}{r^2}\frac{d}{dr}[r(1 - e^{-2\Lambda})] = 8\pi T^{\hat{0}\hat{0}} = 8\pi\rho , \tag{26.35}$$

$$G^{\hat{r}\hat{r}} = -\frac{1}{r^2}(1 - e^{-2\Lambda}) + \frac{2}{r}e^{-2\Lambda}\frac{d\Phi}{dr} = 8\pi T^{\hat{r}\hat{r}} = 8\pi P . \tag{26.36}$$

We can bring these components of the field equation into simpler form by defining a new metric coefficient $m(r)$ by

$$\boxed{e^{2\Lambda} \equiv \frac{1}{1 - 2m/r}} . \tag{26.37}$$

Note [cf. Eqs. (26.1), (26.21), and (26.37)] that outside the star m is equal to the star's total mass-energy M. This, plus the fact that in terms of m the time-time component of the field equation (26.35) takes the form

$$\boxed{\frac{dm}{dr} = 4\pi r^2\rho} , \tag{26.38a}$$

motivates the name *mass inside radius r* for the quantity $m(r)$. In terms of m the radial-radial component (26.36) of the field equation becomes

$$\boxed{\frac{d\Phi}{dr} = \frac{m + 4\pi r^3 P}{r(r - 2m)}} ; \tag{26.38b}$$

and combining this with Eq. (26.34) we obtain an alternative form of the equation of hydrostatic equilibrium

$$\boxed{\frac{dP}{dr} = -\frac{(\rho + P)(m + 4\pi r^3 P)}{r(r - 2m)}} . \tag{26.38c}$$

[This form is called the Tolman-Oppenheimer-Volkoff or TOV equation because it was first derived by Tolman (1939) and first used in a practical calculation by Oppenheimer and Volkoff (1939).] Equations (26.38a), (26.38b), (26.38c) plus an equation of state for the pressure of the stellar material P in terms of its density of total mass-energy ρ,

$$\boxed{P = P(\rho)} , \tag{26.38d}$$

determine the four quantities Φ, m, ρ, and P as functions of radius. In other words, *Eqs. (26.38) are the relativistic equations of stellar structure*

Actually, for full determination, one also needs boundary conditions. Just as the surface of a sphere is everywhere locally Euclidean (i.e., is arbitrarily close to Euclidean in arbitrarily small regions), so also spacetime must be everywhere locally Lorentz; cf. Eqs. (25.9). In order that spacetime be locally Lorentz at the star's center (in particular, that circumferences of tiny circles around the center be equal to 2π times their radii), it is necessary that m vanish at the center

$$m = 0 \quad \text{at } r = 0, \quad \text{and thus} \quad \boxed{m(r) = \int_0^r 4\pi r^2 \rho dr} \; ; \tag{26.39}$$

cf. Eqs. (26.21) and (26.37). At the star's surface the interior spacetime geometry (26.21) must join smoothly to the exterior Schwarzschild geometry (26.1), and hence

$$\boxed{m = M \quad \text{and} \quad e^{2\Phi} = 1 - 2M/r \quad \text{at } r = R} \; . \tag{26.40}$$

26.3.5 Stellar Models and Their Properties

A little thought now reveals a straightforward method of producing a relativistic stellar model: (*i*) Specify an equation of state for the stellar material $P = P(\rho)$ and specify a central density ρ_c or central pressure P_c for the star. (*ii*) Integrate the coupled hydrostatic-equilibrium equation (26.38c) and "mass equation" (26.38a) outward from the center, beginning with the initial conditions $m = 0$ and $P = P_c$ at the center. (*iii*) Terminate the integration when the pressure falls to zero; this is the surface of the star. (*iv*) At the surface read off the value of m; it is the star's total mass-energy M, which appears in the star's external, Schwarzschild line element (26.1). (*v*) From this M and the radius $r \equiv R$ of the star's surface, read off the value of the gravitational potential Φ at the surface [Eq. (26.40)]. (*vi*) Integrate the Einstein field equation (26.38b) inward from the surface toward the center to determine Φ as a function of radius inside the star.

Just six weeks after reading to the Prussian Academy of Science the letter in which Karl Schwarzschild derived his vacuum solution (26.1) of the field equation, Albert Einstein again presented the Academy with results from Schwarzschild's fertile mind: an exact solution for the structure of the interior of a star that has constant density ρ. [And just four months after that, on June 29, 1916, Einstein had the sad task of announcing to the Academy that Schwarzschild had died of an illness contracted on the World-War-I Russian front.]

In our notation, Schwarzschild's solution for the interior of a star is characterized by its uniform density ρ, its total mass M, and its radius R which is given in terms of ρ and M by

$$M = \frac{4\pi}{3}\rho R^3 \tag{26.41}$$

[Eq. (26.39)]. In terms of these, the mass inside radius r, the pressure P, and the gravitational potential Φ are (Schwarzschild 1916b)

$$m = \frac{4\pi}{3}\rho r^3 \;, \quad P = \rho \left[\frac{(1 - 2Mr^2/R^3)^{\frac{1}{2}} - (1 - 2M/R)^{\frac{1}{2}}}{3(1 - 2M/R)^{\frac{1}{2}} - (1 - 2Mr^2/R^3)^{\frac{1}{2}}} \right] \;, \tag{26.42}$$

$$e^{\Phi} = \frac{3}{2}\left(1 - \frac{2M}{R}\right)^{\frac{1}{2}} - \frac{1}{2}\left(1 - \frac{2Mr^2}{R^3}\right)^{\frac{1}{2}} . \qquad (26.43)$$

We present these details less for their specific physical content than to illustrate the solution of the Einstein field equation in a realistic, astrophysically interesting situation. For discussions of the application of this formalism to neutron stars, where relativistic deviations from Newtonian theory can be rather strong, see e.g., Shapiro and Teukolsky (1983). For the seminal work on the theory of neutron-star structure see Oppenheimer and Volkoff (1939).

Among the remarkable consequences of the TOV equation of hydrostatic equilibrium (26.38c) for neutron-star structure are these: (i) If the mass m inside radius r ever gets close to $r/2$, the "gravitational pull" [right-hand side of (26.38c)] becomes divergently large, forcing the pressure gradient that counterbalances it to be divergently large, and thereby driving the pressure quickly to zero as one integrates outward. This protects the static star from having M greater than $R/2$, i.e., from having its surface inside its gravitational radius. (ii) Although the density of matter near the center of a neutron star is above that of an atomic nucleus, where the equation of state is ill-understood, we can be confident that there is an upper limit on the masses of neutron stars, a limit in the range $2M_{\odot} \lesssim M_{\max} \lesssim 3M_{\odot}$. This mass limit cannot be avoided by postulating that a more massive neutron star develops an arbitrarily large central pressure and thereby supports itself against gravitational implosion. The reason is that an arbitrarily large central pressure is self-defeating: The "gravitational pull" which appears on the right-hand side of (26.38c) is quadratic in the pressure at very high pressures (whereas it would be independent of pressure in Newtonian theory). This purely relativistic feature guarantees that if a star develops too high a central pressure, it will be unable to support itself against the resulting "quadratically too high" gravitational pull.

****

EXERCISES

Exercise 26.6 *Challenge: Mass-Radius Relation for Real Neutron Stars*
Choose a physical equation of state from the alternatives presented in Shapiro & Teukolsky (1983) and represent it numerically. Then integrate the TOV equation starting with several suitable central pressures and deduce a mass-radius relation, $M(R)$. You should find that as the central pressure is increased, the mass passes through a maximum while the radius continues to *decrease*. (Solutions with radii smaller than that associated with the maximum mass are unstable to radial perturbations.)

****

26.3.6   Embedding Diagrams

We conclude our discussion of static stars by using them to illustrate a useful technique for visualizing the curvature of spacetime: the embedding of the curved spacetime, or a piece of it, in a flat space of higher dimensionality.

The geometry of a curved, n-dimensional manifold is characterized by $\frac{1}{2}n(n+1)$ metric components (since those components form a symmetric $n \times n$ matrix), of which only $\frac{1}{2}n(n+1) - n = \frac{1}{2}n(n-1)$ are of coordinate-independent significance (since we are free to choose arbitrarily the n coordinates of our coordinate system and can thereby force n of the metric components to take on any desired values, e.g., zero). If this n-dimensional manifold is embedded in a flat N-dimensional manifold, that embedding will be described by expressing $N - n$ of the embedding manifold's Euclidean (or Lorentz) coordinates in terms of the other n. Thus, the embedding will be characterized by $N - n$ functions of n variables. In order for the embedding to be possible, in general, this number of choosable functions must be at least as large as the number of significant metric coefficients $\frac{1}{2}n(n-1)$. From this argument we conclude that *the dimensionality of the embedding space must be $N \geq \frac{1}{2}n(n+1)$*. Actually, this argument analyzes only the local features of the embedding. If one wants also to preserve the global topology of the n-dimensional manifold, one must in general go to an embedding space of even higher dimensionality.

Curved spacetime has $n = 4$ dimensions and thus requires for its local embedding a flat space with $N = 10$ dimensions. This is a bit much for 3-dimensional beings like us to visualize. If, as a sop to our visual limitations, we reduce our ambitions and seek only to extract a 3-surface from curved spacetime and visualize it by embedding it in a flat space, we will require a flat space of $N = 6$ dimensions. This is still a bit much. In frustration we are driven to extract from spacetime $n = 2$ dimensional surfaces and visualize them by embedding in flat spaces with $N = 3$ dimensions. This is doable—and, indeed, instructive.

As a nice example, consider the equatorial "plane" through the spacetime of a static spherical star, at a specific "moment" of coordinate time t; i.e., consider the 2-surface $t = $ const, $\theta = \pi/2$ in the spacetime of Eqs. (26.21), (26.37). The line element on this equatorial 2-surface is

$$^{(2)}ds^2 = \frac{dr^2}{1 - 2m/r} + r^2 d\phi^2 , \quad \text{where} \quad m = m(r) = \int_0^r 4\pi r^2 \rho dr ; \qquad (26.44)$$

cf. Eq. (26.39). We seek to construct in a 3-dimensional Euclidean space a 2-dimensional surface with precisely this same 2-geometry. As an aid, we introduce in the Euclidean embedding space a cylindrical coordinate system $\{r, z, \phi\}$, in terms of which the space's 3-dimensional line element is

$$^{(3)}ds^2 = dr^2 + dz^2 + rd\phi^2 . \qquad (26.45)$$

The surface we seek to embed is axially symmetric, so we can describe its embedding by the value of z on it as a function of radius r: $z = z(r)$. Inserting this (unknown) embedding function into Eq. (26.45), we obtain for the surface's 2-geometry,

$$^{(2)}ds^2 = [1 + (dz/dr)^2]dr^2 + r^2 d\phi^2 ; \qquad (26.46)$$

and comparing with our original expression (26.44) for the 2-geometry we obtain a differential equation for the embedding function:

$$\frac{dz}{dr} = \left(\frac{1}{1 - 2m/r} - 1 \right)^{\frac{1}{2}} . \qquad (26.47)$$
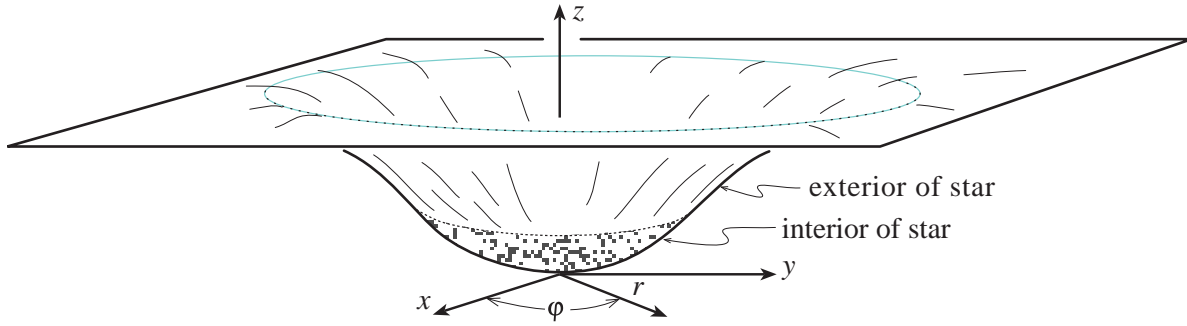
Fig. 26.1: Embedding diagram depicting an equatorial, 2-dimensional slice $t = $ const, $\theta = \pi/2$ through the spacetime of a spherical star with uniform density ρ and with radius R equal to 2.5 times the gravitational radius $2M$. See Ex. 26.7 for details.

If we set $z = 0$ at the star's center, then the solution of this differential equation is

$$z = \int_0^r \frac{dr}{[(r/2m) - 1]^{\frac{1}{2}}} . \tag{26.48}$$

Near the star's center $m(r)$ is given by $m = (4\pi/3)\rho_c r^3$, where ρ_c is the star's central density; and outside the star $m(r)$ is equal to the star's r-independent total mass M. Correspondingly, in these two regions Eq. (26.48) reduces to

$$z = \sqrt{(2\pi/3)\rho_c}\, r^2 \ \ \text{at } r \text{ very near zero} .$$
$$z = \sqrt{8M(r - 2M)} + \text{constant} \ \ \text{at } r > R , \quad \text{i.e., outside the star.} \tag{26.49}$$

Figure 26.1 shows the embedded 2-surface $z(r)$ for a star of uniform density $\rho = $ const; cf. Ex. 26.7. For any other star the embedding diagram will be qualitatively similar, though quantitatively different.

The most important feature of this embedding diagram is its illustration of the fact [also clear in the original line element (26.44)] that, as one moves outward from the star's center, its circumference $2\pi r$ increases less rapidly than the proper radial distance travelled, $l = \int_0^r (1 - 2m/r)^{-\frac{1}{2}} dr$. As a specific example, the distance from the center of the earth to a perfect circle near the earth's surface is more than circumference/2π by about 1.5 millimeters—a number whose smallness compared to the actual radius, 6.4×10^8 cm, is a measure of the weakness of the curvature of spacetime near earth. As a more extreme example, the distance from the center of a massive neutron star to its surface is about one kilometer greater than circumference/2π—i.e., greater by an amount that is roughly 10 percent of the ~ 10 km circumference/2π. Correspondingly, in the embedding diagram for the earth (Fig. 26.1) the embedded surface would be so nearly flat that its downward dip at the center would be noticeable only with great effort; whereas the embedding diagram for a neutron star would show a downward dip about like that of Fig. 26.1.

****

EXERCISES

Exercise 26.7 *Example: Embedding Diagram for Star with Uniform Density*

(a) Show that the embedding surface of Eq. (26.48) is a paraboloid of revolution everywhere outside the star.

(b) Show that in the interior of a uniform-density star, the embedding surface is a segment of a sphere.

(c) Show that the match of the interior to the exterior is done in such a way that, in the embedding space the embedded surface shows no kink (no bend) at $r = R$.

(d) Show that, in general, the circumference/2π for a star is less than the distance from the center to the surface by an amount of order the star's Schwarzschild radius $2M$. Evaluate this amount analytically for a star of uniform density, and numerically (approximately) for the earth and for a neutron star.

****

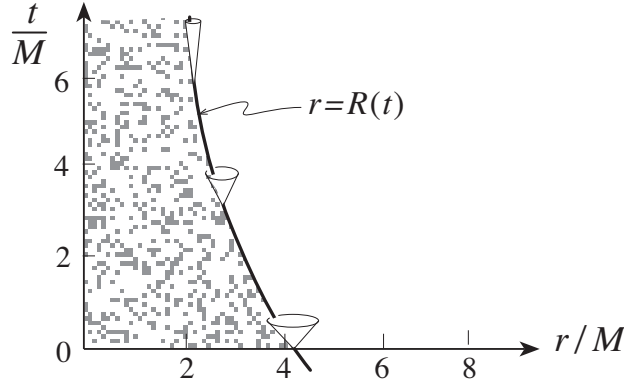# 26.4 Gravitational Implosion of a Star to Form a Black Hole

J. Robert Oppenheimer, upon discovering with his student George Volkoff that there is a maximum mass limit for neutron stars (Oppenheimer and Volkoff 1939), was forced to consider the possibility that, when it exhausts its nuclear fuel, a more massive star will implode to radii $R \leq 2M$. Just before the outbreak of World War II, Oppenheimer and his graduate student Hartland Snyder investigated the details of such an implosion, for the idealized case of a perfectly spherical star in which all the internal pressure is suddenly extinguished; see Oppenheimer and Snyder (1939). In this section we shall repeat their analysis, though from a more modern viewpoint and using somewhat different arguments.[3]

By Birkhoff's theorem, the spacetime geometry outside an imploding, spherical star must be that of Schwarzschild. This means, in particular, that an imploding, spherical star cannot produce any gravitational waves; such waves would break the spherical symmetry. By contrast, a star that implodes nonspherically can produce a strong burst of gravitational waves; see Chap. 27.

Since the spacetime geometry outside an imploding, spherical star is that of Schwarzschild, we can depict the motion of the star's surface by a world line in a 2-dimensional spacetime diagram with Schwarzschild coordinate time t plotted upward and Schwarzschild coordinate radius r plotted rightward (Fig. 26.2). The world line of the star's surface is an ingoing curve. The region to the left of the world line must be discarded and replaced by the spacetime of the star's interior, while the region to the right, $r > R(t)$, is correctly described by Schwarzschild.

---

[3]For further details, see MTW Chapters 31 and 32.

Fig. 26.2: Spacetime diagram depicting in Schwarzschild coordinates the gravitationally induced implosion of a star. The thick solid curve is the world line of the star's surface, $r = R(t)$ in the external Schwarzschild coordinates. The stippled region to the left of that world line is not correctly described by the Schwarzschild line element (26.1); it requires for its description the spacetime metric of the star's interior. The surface's world line $r = R(t)$ is constrained to lie inside the light cones.

As for a static star, so also for an imploding one, because real atoms with finite rest masses live on the star's surface, the world line of that surface, $\{r = R(t), \theta$ and ϕ constant$\}$, must be timelike. Consequently, at each point along the world line it must lie within the local light cones that are depicted in Fig. 26.2.

The radial edges of the light cones are lines along which the Schwarzschild line element, the ds^2 of Eq. (26.1), vanishes with θ and ϕ held fixed:

$$0 = ds^2 = -(1 - 2M/R)dt^2 + \frac{dr^2}{1 - 2M/R} \;;\quad \text{i.e.,} \quad \frac{dt}{dr} = \pm\frac{1}{1 - 2M/R} \cdot \qquad (26.50)$$

Therefore, instead of having 45-degree opening angles $dt/dr = \pm 1$ as they do in a Lorentz frame of flat spacetime, the light cones "squeeze down" toward $dt/dr = \infty$ as the star's surface $r = R(t)$ approaches the gravitational radius, $R \to 2M$. This is a peculiarity due not to spacetime curvature, but rather to the nature of the Schwarzschild coordinates: If, at any chosen event of the Schwarzschild spacetime, we were to introduce a local Lorentz frame, then in that frame the light cones would have 45-degree opening angles.

Since the world line of the star's surface is confined to the interiors of the local light cones, *the squeezing down of the light cones near $r = 2M$ prevents the star's world line $r = R(t)$ from ever, in any finite coordinate time t, reaching the gravitational radius, $r = 2M$.*

This conclusion is completely general; it relies in no way whatsoever on the details of what is going on inside the star or at its surface. It is just as valid for completely realistic stellar implosion (with finite pressure and shock waves) as for the idealized, Oppenheimer-Snyder case of zero-pressure implosion. In the special case of zero pressure, one can explore the details further:

Because no pressure forces act on the atoms at the star's surface, those atoms must move inward along radial geodesic world lines. Correspondingly, the world line of the star's surface in the external Schwarzschild spacetime must be a timelike geodesic of constant (θ, ϕ). In Ex. 26.8 the geodesic equation is solved to determine that world line $R(t)$, with a conclusion

that agrees with the above argument: *Only after a lapse of infinite coordinate time t does the star's surface reach the gravitational radius $r = 2M$.* A byproduct of that calculation is equally remarkable: Although the implosion to $R = 2M$ requires infinite Schwarzschild coordinate time t, it requires only a finite proper time τ as measured by an observer who rides inward on the star's surface. In fact, the proper time is

$$\boxed{\tau \simeq \frac{\pi}{2}\left(\frac{R_o^3}{2M}\right)^{\frac{1}{2}} = 15\,\text{microseconds}\left(\frac{R_o}{2M}\right)^{3/2}\frac{M}{M_\odot} \quad \text{if } R_o \gg 2M} , \qquad (26.51)$$

where R_o is the star's initial radius when it first begins to implode freely, $M_\odot$ denotes the mass of the sun, and proper time τ is measured from the start of implosion. Note that this implosion time is equal to $1/(4\sqrt{2})$ times the orbital period of a test particle at the radius of the star's initial surface. For a star with mass and initial radius equal to those of the sun, τ is about 30 minutes; for a neutron star that has been pushed over the maximum mass limit by accretion of matter from its surroundings, τ is about 0.1 milliseconds.

26.4.1   Tidal Forces at the Gravitational Radius

What happens to the star's surface, and an observer on it, when—after infinite coordinate time but tiny proper time—it reaches the gravitational radius? There are two possibilities: (i) the tidal gravitational forces there might be so strong that they destroy the star's surface and any observers on it; or, (ii) if the tidal forces are not that strong, then the star and observers must continue to exist, moving into a region of spacetime (presumably $r < 2M$) that is not smoothly joined onto $r > 2M$ in the Schwarzschild coordinate system. In the latter case, the pathology is all due to poor properties of Schwarzschild's coordinates. In the former case, it is due to an intrinsic, coordinate-independent singularity of the tide-producing Riemann curvature.

To see which is the case, we must evaluate the tidal forces felt by observers on the surface of the imploding star. Those tidal forces are produced by the Riemann curvature tensor. More specifically, if an observer's feet and head have a vector separation $\boldsymbol{\xi}$ at time τ as measured by the observer's clock, then the curvature of spacetime will exert on them a relative gravitational acceleration given by the equation of geodesic deviation, in the form appropriate to a local Lorentz frame:

$$\frac{d^2\xi^{\bar{j}}}{d\tau^2} = -R^{\bar{j}}{}_{\bar{0}\bar{k}\bar{0}}\xi^{\bar{k}} \qquad (26.52)$$

[Eq. (25.31)]. Here the barred indices denote components in the observer's local Lorentz frame. The tidal forces will become infinite, and will thereby destroy the observer and all forms of matter on the star's surface, if and only if the local Lorentz Riemann components $R_{\bar{j}\bar{0}\bar{k}\bar{0}}$ diverge as the star's surface approaches the gravitational radius. Thus, to test whether the observer and star survive, we must compute the components of the Riemann curvature tensor in the local Lorentz frame of the star's imploding surface.

The easiest way to compute those components is by a transformation from components as measured in the proper reference frames of observers who are "at rest" (fixed r, θ, ϕ) in

the Schwarzschild spacetime. At each event on the world tube of the star's surface, then, we have two orthonormal frames: one (barred indices) a local Lorentz frame imploding with the star; the other (hatted indices) a proper reference frame at rest. Since the metric coefficients in these two bases have the standard flat-space form $g_{\bar{\alpha}\bar{\beta}} = \eta_{\alpha\beta}$, $g_{\hat{\alpha}\hat{\beta}} = \eta_{\alpha\beta}$, the bases must be related by a Lorentz transformation [cf. Eq. (2.36b) and associated discussion]. A little thought makes it clear that the required transformation matrix is that for a pure boost [Eq. (2.38a)]

$$L^{\hat{0}}{}_{\bar{0}} = L^{\hat{r}}{}_{\bar{r}} = \gamma , \quad L^{\hat{0}}{}_{\bar{r}} = L^{\hat{r}}{}_{\bar{0}} = -\beta\gamma , \quad L^{\hat{\theta}}{}_{\bar{\theta}} = L^{\hat{\phi}}{}_{\bar{\phi}} = 1 ; \quad \gamma = \frac{1}{\sqrt{1-\beta^2}} , \qquad (26.53)$$

with β the speed of implosion of the star's surface, as measured in the proper reference frame of the static observer when the surface flies by. The transformation law for the components of the Riemann tensor has, of course, the standard form for any fourth rank tensor:

$$R_{\bar{\alpha}\bar{\beta}\bar{\gamma}\bar{\delta}} = L^{\hat{\mu}}{}_{\bar{\alpha}} L^{\hat{\nu}}{}_{\bar{\beta}} L^{\hat{\lambda}}{}_{\bar{\gamma}} L^{\hat{\sigma}}{}_{\bar{\delta}} R_{\hat{\mu}\hat{\nu}\hat{\lambda}\hat{\sigma}} . \qquad (26.54)$$

The basis vectors of the proper reference frame are given by Eq. (4) of Box 26.2, and from that Box we learn that the components of Riemann in this basis are:

$$R_{\hat{0}\hat{r}\hat{0}\hat{r}} = -\frac{2M}{R^3} , \quad R_{\hat{0}\hat{\theta}\hat{0}\hat{\theta}} = R_{\hat{0}\hat{\phi}\hat{0}\hat{\phi}} = +\frac{M}{R^3} ,$$

$$R_{\hat{\theta}\hat{\phi}\hat{\theta}\hat{\phi}} = \frac{2M}{R^3} , \quad R_{\hat{r}\hat{\theta}\hat{r}\hat{\theta}} = R_{\hat{r}\hat{\phi}\hat{r}\hat{\phi}} = -\frac{M}{R^3} . \qquad (26.55)$$

These are the components measured by static observers.

By inserting these static-observer components and the Lorentz-transformation matrix (26.53) into the transformation law (26.54) we reach our goal: The following components of Riemann in the local Lorentz frame of the star's freely imploding surface:

$$R_{\bar{0}\bar{r}\bar{0}\bar{r}} = -\frac{2M}{R^3} , \quad R_{\bar{0}\bar{\theta}\bar{0}\bar{\theta}} = R_{\bar{0}\bar{\phi}\bar{0}\bar{\phi}} = +\frac{M}{R^3} ,$$

$$R_{\bar{\theta}\bar{\phi}\bar{\theta}\bar{\phi}} = \frac{2M}{R^3} , \quad R_{\bar{r}\bar{\theta}\bar{r}\bar{\theta}} = R_{\bar{r}\bar{\phi}\bar{r}\bar{\phi}} = -\frac{M}{R^3} . \qquad (26.56)$$

These components are remarkable in two ways: First, they remain perfectly finite as the star's surface approaches the gravitational radius, $R \to 2M$; and, correspondingly, tidal gravity cannot destroy the star or the observers on its surface. Second, the components of Riemann are identically the same in the two orthonormal frames, hatted and barred, which move radially at finite speed β with respect to each other [expressions (26.56) are independent of β and are the same as (26.55)]. This is a result of the very special algebraic structure that Riemann's components have for the Schwarzschild spacetime; it will not be true in typical spacetimes.

26.4.2   Stellar Implosion in Eddington-Finklestein Coordinates

From the finiteness of the components of Riemann in the surface's local Lorentz frame, we conclude that something must be wrong with Schwarzschild's t, r, θ, ϕ coordinate system in

the vicinity of the gravitational radius $r = 2M$: Although nothing catastrophic happens to the star's surface as it approaches $2M$, those coordinates refuse to describe passage through $r = 2M$ in a reasonable, smooth, finite way. Thus, in order to study the implosion as it passes through the gravitational radius and beyond, we shall need a new, improved coordinate system.

Several coordinate systems have been devised for this purpose. For a study and comparison of them see, e.g., Chap. 31 of MTW. In this chapter we shall confine ourselves to one: A coordinate system devised for other purposes by Arthur Eddington (1922), then long forgotten and only rediscovered independently and used for this purpose by David Finkelstein (1958). Yevgeny Lifshitz, of Landau-Lifshitz fame, told one of the authors many years later what an enormous impact Finkelstein's coordinate system had on peoples' understanding of the implosion of stars. "You cannot appreciate how difficult it was for the human mind before Finkelstein to understand [the Oppenheimer-Snyder analysis of stellar implosion]." Lifshitz said. When, nineteen years after Oppenheimer and Snyder, the issue of the Physical Review containing Finkelstein's paper arrived in Moscow, suddenly everything was clear.

Finkelstein, a postdoctoral fellow at the Stevens Institute of Technology in Hoboken, New Jersey, found the following simple transformation which moves the region $t = \infty$, $r = 2M$ of Schwarzschild coordinates in to a finite location. His transformation involves introducing a new time coordinate

$$\tilde{t} = t + 2M \ln |(r/2M) - 1| , \tag{26.57}$$

but leaving unchanged the radial and angular coordinates. Figure 26.3 shows the surfaces of constant Eddington-Finkelstein time $\tilde{t}$ in Schwarzschild coordinates, and the surfaces of constant Schwarzschild time t in Eddington-Finkelstein coordinates. Notice, as advertised, that $t = \infty$, $r = 2M$ is moved to a finite Eddington-Finkelstein location.

By inserting the coordinate transformation (26.57) into the Schwarzschild line element (26.1) we obtain the following line element for Schwarzschild spacetime written in Eddington-
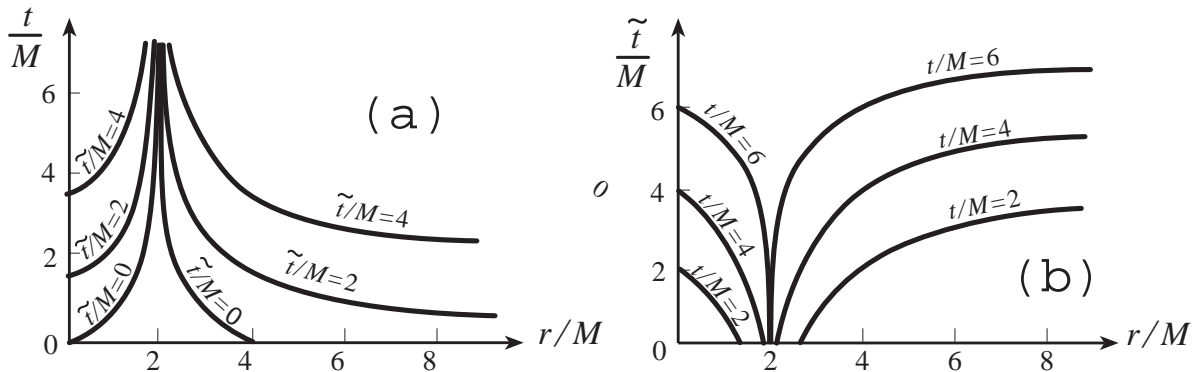
Fig. 26.3: (a) The 3-surfaces of constant Eddington-Finkelstein time coordinate $\tilde{t}$ drawn in a Schwarzschild spacetime diagram, with the angular coordinates θ, ϕ suppressed. (b) The 3-surfaces of constant Schwarzschild time coordinate t drawn in an Eddington-Finkelstein spacetime diagram, with angular coordinates suppressed.
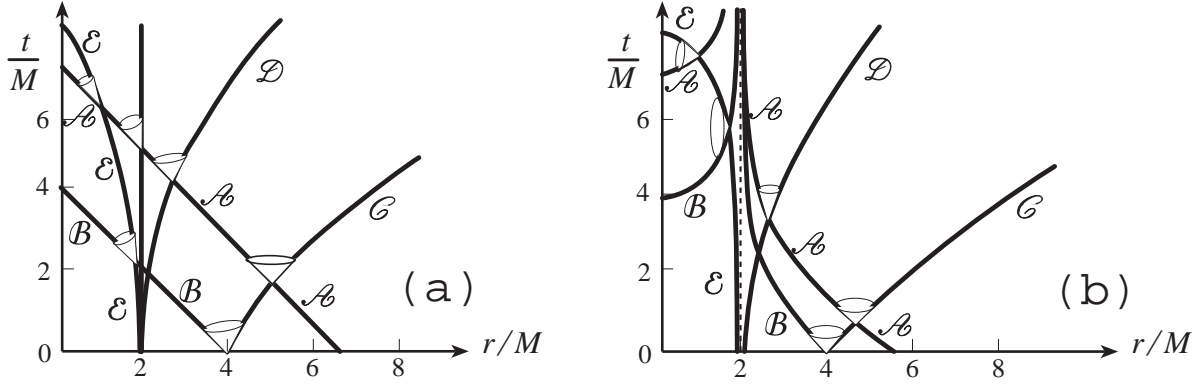
Fig. 26.4: (a) Radial light rays, and light cones, for the Schwarzschild spacetime as depicted in Eddington-Finkelstein coordinates [Eq. (26.59)]. (b) These same light rays and light cones as depicted in Schwarzschild coordinates [cf. Fig. **??**].

Finkelstein coordinates:

$$ds^2 = -\left(1 - \frac{2M}{r}\right)d\tilde{t}^2 + \frac{4M}{r}d\tilde{t}\,dr + \left(1 + \frac{2M}{r}\right)dr^2 + r^2(d\theta^2 + \sin^2\theta d\phi^2)\right]. \quad (26.58)$$

Notice that, by contrast with the line element in Schwarzschild coordinates, none of the metric coefficients diverge as r approaches $2M$. Moreover, in an Eddington-Finkelstein spacetime diagram, by contrast with Schwarzschild, the light cones do not pinch down to slivers at $r = 2M$ [compare Figs. 26.4a and 26.4b]: The world lines of radial light rays are computable in Eddington-Finkelstein, as in Schwarzschild, by setting $ds^2 = 0$ (null world lines) and $d\theta = d\phi = 0$ (radial world lines) in the line element. The result, depicted in Fig. 26.4a, is

$$\frac{d\tilde{t}}{dr} = -1 \text{ for ingoing rays; and } \frac{d\tilde{t}}{dr} = \left(\frac{1 + 2M/r}{1 - 2M/r}\right) \text{ for outgoing rays.} \quad (26.59)$$

Note that, in the Eddington-Finklestein coordinate system, the ingoing light rays plunge unimpeded through $r = 2M$ and in to $r = 0$ along 45-degree lines. The outgoing light rays, by contrast, are never able to escape outward through $r = 2M$: Because of the inward tilt of the outer edge of the light cone, all light rays that begin inside $r = 2M$ are forced forever to remain inside, and in fact are drawn inexorably into $r = 0$, whereas light rays initially outside $r = 2M$ can escape to $r = \infty$.

Return, now, to the implosion of a star. The world line of the star's surface, which became asymptotically frozen at the gravitational radius when studied in Schwarzschild coordinates, plunges unimpeded through $r = 2M$ and into $r = 0$ when studied in Eddington-Finkelstein coordinates; see Ex. 26.8 and compare Figs. 26.5b and 26.5a. Thus, in order to understand the star's ultimate fate, we must study the region $r = 0$.

26.4.3 Tidal Forces at $r = 0$ — The Central Singularity

As with $r = 2M$ there are two possibilities: Either the tidal forces as measured on the star's surface remain finite there, in which case something must be going wrong with the coordinate
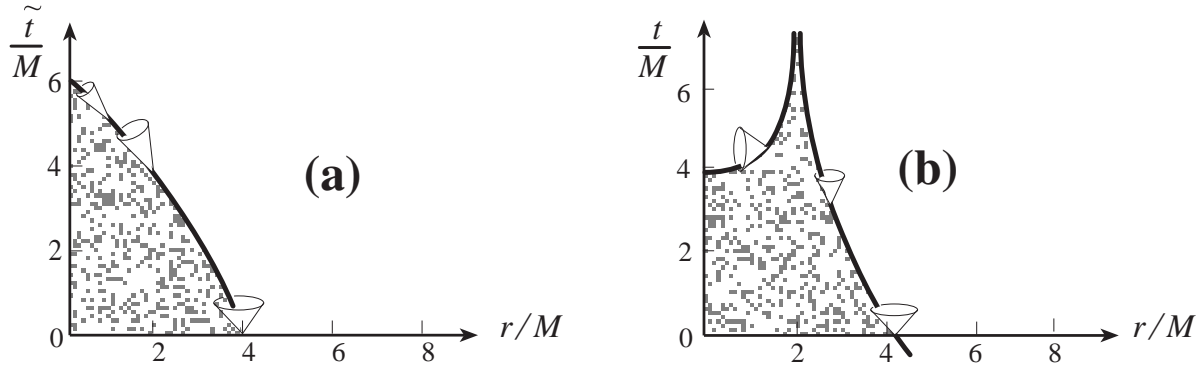
Fig. 26.5: World line of an observer on the surface of an imploding star, as depicted (a) in an Eddington-Finkelstein spacetime diagram, and (b) in a Schwarzschild spacetime diagram; see Ex. 26.8.

system; or else the tidal forces diverge, destroying the star. The tidal forces are computed in Ex. 26.9, with a remarkable result: They diverge. Thus, the region $r = 0$ is a *spacetime singularity*: a region where tidal gravity becomes infinitely large, destroying everything that falls into it.

This, of course, is a very unsatisfying conclusion. It is hard to believe that the correct laws of physics will predict such total destruction. In fact, they probably do not. As we shall discuss in Chap. 28, when the radius of curvature of spacetime becomes as small as $l_{\rm PW} \equiv (G\hbar/c^3)^{\frac{1}{2}} = 10^{-33}$ centimeters, space and time must cease to exist as classical entities; they, and the spacetime geometry must then become quantized; and, correspondingly, general relativity must then break down and be replaced by a quantum theory of the structure of spacetime, i.e., a quantum theory of gravity. That quantum theory will describe and govern the classically singular region at $r = 0$. Since, however, only rough hints of the structure of that quantum theory are in hand at this time, it is not known what that theory will say about the endpoint of stellar implosion.

26.4.4 Schwarzschild Black Hole

Unfortunately, the singularity and its quantum mechanical structure are totally invisible to observers in the external universe: The only way the singularity can possibly be seen is by means of light rays, or other signals, that emerge from its vicinity. However, because the future light cones are all directed into the singularity (Fig. 26.5), no light-speed or sub-light-speed signals can ever emerge from it. In fact, because the outer edge of the light cone is tilted inward at every event inside the gravitational radius (Figs. 26.4 and 26.5), no signal can emerge from inside the gravitational radius to tell external observers what is going on there. In effect, the gravitational radius is an *absolute event horizon* for our universe, a horizon beyond which we cannot see—except by plunging through it, and paying the ultimate price for our momentary exploration of the hole's interior: we cannot publish the results of our observations.

As most readers are aware, the region of strong, vacuum gravity left behind by the implosion of the star is called a *black hole*. The horizon, $r = 2M$, is the surface of the hole,
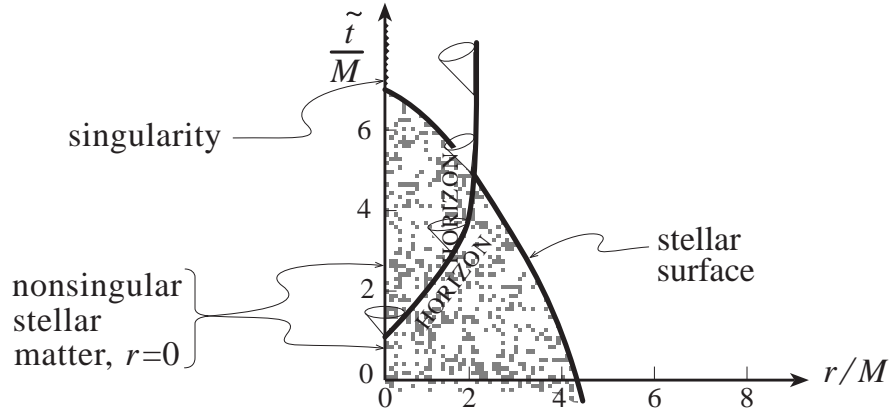
Fig. 26.6: Spacetime diagram depicting the formation and evolution of the horizon of a black hole. The coordinates outside the surface of the imploding star are those of Eddington and Finkelstein; those inside are a smooth continuation of Eddington and Finkelstein (not explored in this book). Note that the horizon is the boundary of the region that is unable to send outgoing null geodesics to radial infinity.

and the region $r < 2M$ is its interior. The spacetime geometry of the black hole, outside and at the surface of the star which creates it by implosion, is that of Schwarzschild—though, of course, Schwarzschild had no way of knowing this in the few brief months left to him after his discovery of the Schwarzschild line element.

The horizon—defined as the boundary between spacetime regions that can and cannot communicate with the external universe—actually forms initially at the star's center, and then expands to encompass the star's surface at the precise moment when the surface penetrates the gravitational radius. This evolution of the horizon is depicted in an Eddington-Finkelstein-type spacetime diagram in Fig. 26.6.

Our discussion here has been confined to spherically symmetric, nonrotating black holes created by the gravitational implosion of a spherically symmetric star. Real stars, of course, are not spherical; and it was widely believed—perhaps we should say hoped—in the 1950s and 1960s that black-hole horizons and singularities would be so unstable that small nonsphericities or small rotation of the imploding star would save it from the black-hole fate. However, elegant and very general analyses carried out in the 1960s, largely by the British physicists Roger Penrose and Stephen Hawking, showed otherwise; and more recent numerical simulations on supercomputers have confirmed those analyses: Singularities are a generic outcome of stellar implosion, as are the black-hole horizons that clothe them.

****

EXERCISES

Exercise 26.8 *Example: Implosion of the Surface of a Zero-Pressure Star*
Consider the surface of a zero-pressure star, which implodes along a timelike geodesic $r = R(t)$ in the Schwarzschild spacetime of its exterior. Analyze that implosion using Schwarzschild coordinates t, r, θ, ϕ, and the exterior metric (26.1) in those coordinates.

(a) Show, using the result of Ex. 25.4a, that the covariant time component u_t of the 4-velocity $\vec{u}$ of a particle on the star's surface is conserved along its world line. Evaluate this conserved quantity in terms of the star's mass M and the radius $r = R_o$ at which it begins to implode.

(b) Use the normalization of the 4-velocity to show that the star's radius R as a function of the proper time τ since implosion began (proper time as measured on its surface) satisfies the differential equation

$$\frac{dR}{d\tau} = -[\text{const} + 2M/R]^{\frac{1}{2}} ; \qquad (26.60)$$

and evaluate the constant. Compare this with the equation of motion for the surface as predicted by Newtonian gravity, with proper time τ replaced by Newtonian time. (It is a coincidence that the two equations are identical.)

(c) Show from the equation of motion (26.60) that the star implodes through the horizon $R = 2M$ in a finite proper time of order (26.51). Show that this proper time has the magnitudes cited in Eq. (26.51) and the sentences following it.

(d) Show that the Schwarzschild coodinate time t required for the star to reach its gravitational radius $R \to 2M$ is infinite.

(e) Show, further, that when studied in Eddington-Finkelstein coordinates, the surface's implosion to $R = 2M$ requires only finite coordinate time $\tilde{t}$; in fact, a time of the same order of magnitude as the proper time (26.51). [Hint: from the Eddington-Finkelstein line element (26.58) and Eq. (26.51) derive a differential equation for $d\tilde{t}/d\tau$ along the world line of the star's surface, and use it to examine the behavior of $d\tilde{t}/d\tau$ near $R = 2M$.] Show, further, that expression (26.60) remains valid all the way through the gravitational radius and in to $r = 0$. From this conclude that the proper time and Eddington-Finkelstein time to reach $r = 0$ are also of order (26.51).

(f) Show that the world line of the star's surface as depicted in an Eddington-Finkelstein spacetime diagram has the form shown in Fig. 26.5a, and that in a Schwarzschild spacetime diagram it has the form shown in 26.5b.

Exercise 26.9 *Example: Gore at the Singularity*

(a) Knowing the world line of the surface of an imploding star in Eddington-Finkelstein coordinates, draw that world line in a Schwarzschild spacetime diagram. Note that, as the world line approaches $r = 0$, it asymptotes to the curve $\{(t, \theta, \phi) = \text{const}, r \text{ variable}\}$. Explain why this is required by the light-cone structure near $r = 0$.

(b) Show that the curve to which it asymptotes, $\{(t, \theta, \phi) = \text{const}, r \text{ variable}\}$ is a timelike geodesic for $r < 2M$. [*Hint:* use the result of Ex. 25.4a.]

(c) Show that the basis vectors of the infalling observer's local Lorentz frame near $r = 0$ are related to the Schwarzschild coordinate basis by

$$\vec{e}_{\hat{0}} = -\left(\frac{2M}{r} - 1\right)^{\frac{1}{2}} \frac{\partial}{\partial r} \,, \quad \vec{e}_{\hat{1}} = \left(\frac{2M}{r} - 1\right)^{-\frac{1}{2}} \frac{\partial}{\partial t} \,, \quad \vec{e}_{\hat{2}} = \frac{1}{r} \frac{\partial}{\partial \theta} \,, \quad \vec{e}_{\hat{3}} = \frac{1}{r \sin \theta} \frac{\partial}{\partial \phi} \,.$$
(26.61)

What are the components of the Riemann tensor in that local Lorentz frame?

(d) Show that the tidal forces produced by the Riemann tensor stretch an infalling observer in the radial, $\vec{e}_{\hat{1}}$, direction and squeeze the observer in the tangential, $\vec{e}_{\hat{2}}$ and $\vec{e}_{\hat{3}}$, directions; and show that the stretching and squeezing forces become infinitely strong as the observer approaches $r = 0$.

(e) Idealize the body of an infalling observer to consist of a head of mass $\mu \simeq 20$kg and feet of mass $\mu \simeq 20$kg separated by a distance $h \simeq 2$ meters, as measured in the observer's local Lorentz frame, and with the separation direction radial. Compute the stretching force between head and feet, as a function of proper time τ, as the observer falls into the singularity. Assume that the hole has the mass $M = 7 \times 10^9 M_\odot$ which has been measured by astronomical observations for the black hole at the center of the nearest giant elliptical galaxy to our own, the galaxy M87. How long before hitting the singularity (at what proper time τ) does the observer die, if he or she is a human being made of flesh, bone, and blood?

Exercise 26.10 $\boxed{T2}$ *Example: Schwarzschild Wormhole*
Our study of the Schwarzschild solution of Einstein's equations in this chapter has been confined to situations where, at small radii, the Schwarzschild geometry joins onto that of a star—either a static star, or a star that implodes to form a black hole. Suppose, by contrast, that there is no matter anywhere in the Schwarzschild spacetime. To get insight into this situation, construct an embedding diagram for the equatorial 2-surfaces $t = \text{const}$, $\theta = \pi/2$ of the vacuum Schwarzschild spacetime, using as the starting point the line element of such a 2-surface written in isotropic coordinates (Ex. 26.3):

$$^{(2)}ds^2 = \left(1 + \frac{M}{2\bar{r}}\right)^4 (d\bar{r}^2 + \bar{r}^2 d\phi^2) \,.$$
(26.62)

Show that the region $0 < \bar{r} \ll M/2$ is an asymptotically flat space, that the region $\bar{r} \gg M/2$ is another asymptotically flat space, and that these two spaces are connected by a *wormhole* ("bridge," "tunnel") through the embedding space. This exercise, first carried out by Ludwig Flamm (1916) in Vienna just a few months after the discovery of the Schwarzschild solution, reveals that the pure vacuum Schwarzschild spacetime represents a wormhole that connects two different universes—or, with a change of topology, a wormhole that connects two widely separated regions of one universe.

Exercise 26.11 $\boxed{T2}$ *Example: Dynamical Evolution of Schwarzschild Wormhole*
The isotropic-coordinate line element (26.16) describing the spacetime geometry of a Schwarzschild wormhole is independent of the time coordinate t. However, because $g_{tt} = 0$ at the

wormhole's throat, $\bar{r} = M/2$, the proper time $d\tau = \sqrt{-ds^2}$ measured by an observer at rest appears to vanish, which cannot be true. Evidently the isotropic coordinates are ill behaved at the throat.

(a) Martin Kruskal (1960) and George Szekeres (1960) have introduced a coordinate system that covers the wormhole's entire spacetime and elucidates its dynamics in a nonsingular manner. The Kruskal-Szekeres time and radial space coordinates v and u are related to the Schwarzschild t and r by

$$(r/2M - 1)e^{r/4M} = u^2 - v^2 \,, \tag{26.63}$$
$$t = 4M \tanh^{-1}(v/u) \quad \text{at } r > 2M \,, \quad t = 4M \tanh^{-1}(u/v) \quad \text{at } r < 2M \,.$$

Show that the metric of Schwarzschild spacetime written in these Kruskal-Szekeres coordinates is

$$ds^2 = (32M^3/r)e^{-r/2M)}(-dv^2 + du^2) + r^2(d\theta^2 + \sin^2\theta d\phi^2) \,, \tag{26.64}$$

where $r(u, v)$ is given by Eq. (26.63).

(b) Draw a spacetime diagram with v increasing upward and u increasing horizontally and rightward. Show that the radial light cones are 45 degree lines everywhere. Show that there are two $r = 0$ singularities, one on the past hyperbola $v = -\sqrt{1 - u^2}$ and the other on the future hyperbola $v = +\sqrt{1 - u^2}$. Show that the gravitational radius $r = 2M$ is at $v = \pm u$. Show that our universe, outside the wormhole, is at $u \gg 1$, and there is another universe at $u \ll -1$.

(c) Draw embedding diagrams for a sequence of spacelike hypersurfaces, the first of which hits the past singularity and the last of which hits the future singularity. Thereby show that the metric (26.64) represents a wormhole that is created in the past, expands to maximum throat circumference $4M$, then pinches off in the future to create a pair of singularities, one in each universe.

(d) Show that nothing can pass through the wormhole from one universe to the other; anything that tries gets crushed in the wormhole's pinch off.

For a Solution, See Fuller and Wheeler (1962), or MTW Chap. 31. For discussions of what is required to hold a wormhole open so it can be traversed, see Morris and Thorne (1988); and for discussions of whether arbitrarily advanced civilizations can create wormholes and hold them open for interstellar travel, and the non-technical discussions and technical references in Everett and Roman (2012). For a discussion of the possible use of traversable wormholes for backward time travel, see Sec. 2.9 of this textbook, and also Everett and Roman (2012) and references therein.

****

26.5 Spinning Black Holes: The Kerr Spacetime

26.5.1 The Kerr Metric for a Spinning Black Hole

Consider a star implodes collapses to form a black hole, and assume for pedagogical simplicity that during the implosion no energy, momentum, or angular momentum flows through a large sphere surrounding the star. Then the asymptotic conservation laws discussed in Sec. 25.9.4 guarantee that the mass M, linear momentum P_j, and angular momentum S_j of the newborn hole, as encoded in its asymptotic metric, will be identical to those of its parent star. If (as we shall assume) our asymptotic coordinates are those of the star's rest frame so $P_j = 0$, then the hole will also be at rest in those coordinates, i.e. it will also have $P_j = 0$.

If the star was non-spinning so $S_j = 0$, then the hole will also have $S_j = 0$, and a powerful theorem due to Werner Israel guarantees that—after it has settled down into a quiescent state—the hole's spacetime geometry will be that of Schwarzschild.

If, instead, the star was spinning so $S_j \neq 0$, then the final, quiescent hole cannot be that of Schwarzschild. Instead, according to a powerful theorem due to Hawking, Carter, Robinson, and others, its spacetime geometry will be the following exact, vacuum solution to the Einstein field equation (which is called the *Kerr solution* because it was discovered by the New-Zealand mathematician Roy Kerr[4]):

$$ds^2 = -\alpha^2 dt^2 + \frac{\rho^2}{\Delta}dr^2 + \rho^2 d\theta^2 + \varpi^2(d\phi - \omega dt)^2 \ . \qquad (26.65a)$$

Here

$$\Delta = r^2 + a^2 - 2Mr \ , \quad \rho^2 = r^2 + a^2 \cos^2\theta \ , \quad \Sigma^2 = (r^2 + a^2)^2 - a^2 \Delta \sin^2\theta \ ,$$

$$\alpha^2 = \frac{\rho^2}{\Sigma^2}\Delta \ , \quad \varpi^2 = \frac{\Sigma^2}{\rho^2}\sin^2\theta \ , \quad \omega = \frac{2aMr}{\Sigma^2} \ . \qquad (26.65b)$$

In this line element $\{t, r, \theta, \phi\}$ are the coordinates, and there are two constants, M and a. The physical meanings of M and a can be deduced from the asymptotic form of this Kerr metric at large radii:

$$ds^2 = -\left(1 - \frac{2M}{r}\right)dt^2 - \frac{4Ma}{r}\sin^2\theta d\phi dt + \left[1 + \mathcal{O}\left(\frac{M}{r}\right)\right][dr^2 + r^2(d\theta^2 + \sin^2\theta d\phi^2)] \ .$$
$$(26.66)$$

By comparing with the standard asymptotic metric in spherical coordinates, Eq. (25.89d), we see that M is the mass of the black hole, $Ma \equiv J_H$ is the magnitude of its spin angular momentum, and its spin points along the polar axis, $\theta = 0$. Evidently, then, the constant a is the hole's angular momentum per unit mass; it has the same dimensions as M: length (in geometrized units).

It is easy to verify that, in the limit $a \to 0$, the Kerr metric (26.65) reduces to the Schwarzschild metric (26.1), and the coordinates $\{t, r, \theta, \phi\}$ in which we have written it (called "Boyer-Lindquist coordinates") reduce to Schwarzschild's coordinates.

---

[4]Kerr, R. P. 1963 Phys Rev. Lett. 11, 237.

Just as it is convenient to read the covariant metric components $g_{\alpha\beta}$ off the line element (26.65a) via $ds^2 = g_{\alpha\beta}dx^\alpha dx^\beta$, so also it is convenient to read the contravariant metric components $g^{\alpha\beta}$ off an expression for the wave operator $\Box \equiv \vec{\nabla} \cdot \vec{\nabla} = g^{\alpha\beta}\nabla_\alpha\nabla_\beta$. (Here $\nabla_\alpha \equiv \nabla_{\vec{e}_\alpha}$ is the directional derivative along the basis vector $\vec{e}_\alpha$.) For the Kerr metric (26.65a), a straightforward inversion of the matrix $||g_{\alpha\beta}||$ gives the $||g^{\alpha\beta}||$ embodied in the following equation:

$$\Box = \frac{-1}{\alpha^2}(\nabla_t + \omega\nabla_\phi)^2 + \frac{\Delta}{\rho^2}\nabla_r{}^2 + \frac{1}{\rho^2}\nabla_\theta{}^2 + \frac{1}{\varpi^2}\nabla_\phi{}^2 . \tag{26.67}$$

26.5.2 Dragging of Inertial Frames

As we saw in Sec. 25.9.3, the angular momentum of a weakly gravitating body can be measured by its frame-dragging, precessional influence on the orientation of gyroscopes. Because the asymptotic metric (26.66) of a Kerr black hole is identical to the weak-gravity metric used to study gyroscopic precession in Sec. 25.9.3, the black hole's spin angular momentum J_{BH} can also be measured via frame-dragging gyroscopic precession.

This frame dragging also shows up in the geodesic trajectories of freely falling particles. Consider, for concreteness, a particle dropped from rest far outside the black hole. Its initial 4-velocity will be $\vec{u} = \partial/\partial t$, and correspondingly, in the distant, flat region of spacetime, the covariant components of $\vec{u}$ will be $u_t = -1$, $u_r = u_\theta = u_\phi = 0$.

Now, the Kerr metric coefficients $g_{\alpha\beta}$, like those of Schwarzschild, are independent of t and ϕ; i.e., the Kerr metric is symmetric under time translation (it is "stationary") and under rotation about the hole's spin axis (it is "axially symmetric"). These symmetries impose corresponding conservation laws on the infalling particle [Ex. 25.4(a)]: u_0 and u_ϕ are conserved;, i.e. they retain their initial values $u_0 = -1$ and $u_\phi = 0$ as the particle falls. By raising indices, $u^\alpha = g^{\alpha\beta}u_\beta$, using the metric coefficients embodied in Eq. (26.67), we learn the evolution of the contravariant 4-velocity components, $u^t = -g^{tt} = 1/\alpha^2$, $u^\phi = -g^{t\phi} = \omega/\alpha^2$. These in turn imply that as the particle falls, it acquires an *angular velocity* around the hole's spin axis given by

$$\Omega \equiv \frac{d\phi}{dt} = \frac{d\phi/d\tau}{dt/d\tau} = \frac{u^\phi}{u^t} = \omega . \tag{26.68}$$

(The coordinates ϕ and t are tied to the rotational and time-translation symmetries of the spacetime, so they are very special; that is why we can use them to define a physically meaningful angular velocity.)

At large radii, $\omega = 2aM/r^3 \to 0$ as $r \to \infty$. Therefore, when first dropped, the particle falls radially inward. However, as the particle nears the hole and picks up speed, it acquires a significant angular velocity around the hole's spin axis. The physical cause of this is *frame dragging:* The hole's spin drags inertial frames into rotation around the spin axis, and that inertial rotation drags the inertially falling particle into a circulatory orbital motion.

26.5.3 The Light-Cone Structure, and the Horizon

Just as for a Schwarzschild hole, so also for Kerr, the light-cone structure is a powerful tool for identifying the horizon and exploring the spacetime geometry near it.

At any event in spacetime, the tangents to the light cone are those displacements $\{dt, dr, d\theta, d\phi\}$ along which $ds^2 = 0$. The outermost and innermost edges of the cone are those for which $(dr/dt)^2$ is maximal. By setting expression (26.65a) to zero we see that dr^2 has its maximum value, for a given dt^2, when $d\phi = \omega dt$ and $d\theta = 0$. In other words, *the photons that move radially outward or inward at the fastest possible rate are those whose angular motion is that of frame dragging*, Eq. (26.68). For these extremal photons, the radial motion (along the outer and inner edges of the light cone) is

$$\frac{dr}{dt} = \pm\frac{\alpha\sqrt{\Delta}}{\rho} = \pm\frac{\Delta}{\Sigma} \ . \tag{26.69}$$

Now, Σ is positive definite, but Δ is not; it decreases monotonically, with decreasing radius, reaching zero at

$$\boxed{r = r_H \equiv M + \sqrt{M^2 - a^2}} \tag{26.70}$$

[Eq. (26.65b)]. (We shall assume that $|a| < M$ so r_H is real, and shall justify this assumption below.) Correspondingly, the light cone closes up to a sliver then pinches off as $r \to r_H$; and it pinches onto a null curve (actually, a null geodesic) given by

$$r = r_H \ , \quad \theta = \text{constant} \ , \quad \phi = \Omega_H t + \text{constant} \ , \tag{26.71}$$

where

$$\boxed{\Omega_H = \omega(r = r_H) = \frac{a}{2Mr_H}} \ . \tag{26.72}$$

This light-cone structure is depicted in Fig. 26.7a,b. The light-cone pinch off as shown there is the same as that for Schwarzschild spacetime (Fig. 26.2) except for the frame-dragging-induced angular tilt $d\phi/dt = \omega$ of the light cones. In the Schwarzschild case, as $r \to 2M$, the light cones pinch onto the geodesic world lines $\{r = 2M, \theta = \text{const}, \phi = \text{const}\}$ of photons that travel along the horizon. These null world lines are called the horizon's *generators*. In the Kerr case, the light-cone pinchoff reveals that *the horizon is at $r = r_H$, and the horizon generators are null geodesics that travel around and around the horizon with angular velocity Ω_H. This motivates us to regard the horizon itself as having the rotational angular velocity Ω_H.*

Whenever a finite-rest-mass particle falls into a spinning black hole, its world line, as it nears the horizon, is constrained always to lie inside the light cone. The light-cone pinch off then constrains its motion to approach, asymptotically, the horizon generators. Therefore, as seen in Boyer-Lindquist coordinates, the particle is dragged into an orbital motion, just above the horizon, with asymptotic angular velocity $d\phi/dt = \Omega_H$, and it travels around and around the horizon "forever" (for infinite Boyer-Lindquist coordinate time t), and never (as $t \to \infty$) manages to cross through the horizon.

As in the Schwarzschild case, so also in Kerr, this infall to $r = r_H$ requires only finite proper time τ as measured by the particle, and the particle feels only finite tidal forces (only
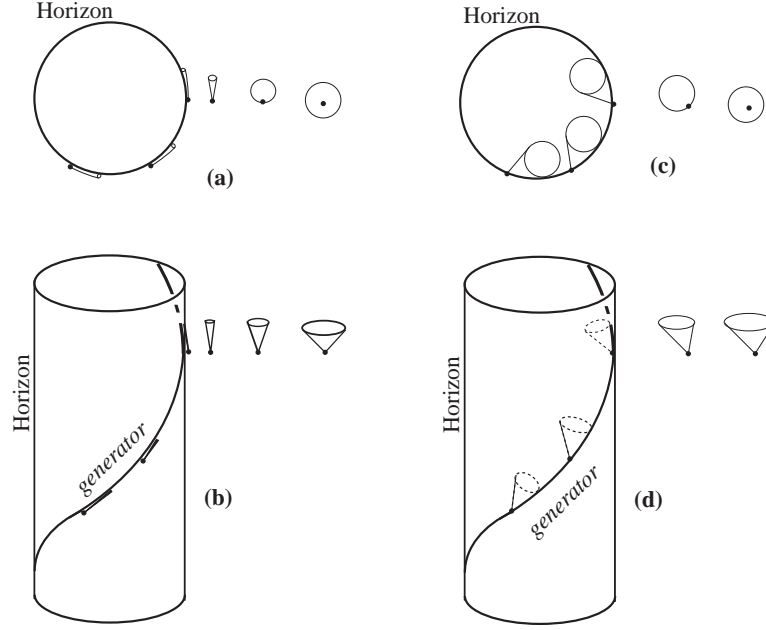
Fig. 26.7: (a) and (b): Light-cone structure of Kerr spacetime depicted in Boyer-Lindquist coordinates. Drawing (b) is a spacetime diagram; drawing (a) is the same diagram as viewed from above. (c) and (d): The same light-cone structure in Kerr coordinates.

finite values of the components of Riemann in its proper reference frame). Therefore, as for Schwarzschild spacetime, the "barrier" to infall through $r = r_H$ must be an illusion produced by a pathology of the Boyer-Lindquist coordinates at $r = r_H$.

This coordinate pathology can be removed by a variety of different coordinate transformations. One is the following change of the time and angular coordinates:

$$\tilde{t} = t + \int \frac{2Mr}{\Delta} dr , \quad \tilde{\phi} = \phi + \int \frac{a}{\Delta} dr .$$

$$(26.73)$$

The new (tilded) coordinates are a variant of a coordinate system originally introduced by Kerr, so we shall call them "Kerr coordinates". By inserting the coordinate transformation (26.73) into the line element (26.65a), we obtain the following form of the Kerr metric, in Kerr coordinates:

$$ds^2 = -\alpha^2 d\tilde{t}^2 + \frac{4Mr\rho^2}{\Sigma^2} dr d\tilde{t} + \frac{\rho^2(\rho^2 + 2Mr)}{\Sigma^2} dr^2 + \rho^2 d\theta^2 + \varpi^2 \left[d\tilde{\phi} - \omega d\tilde{t} - \frac{a(\rho^2 + 2Mr)}{\Sigma^2} dr \right]^2 .$$

$$(26.74)$$

It is easy to verify that, when $a \to 0$ (so Kerr spacetime becomes Schwarzschild), the Kerr coordinates (26.73) become those of Eddington and Finkelstein [Eq. (26.57)], and the Kerr line element (26.74) becomes the Eddington-Finkelstein one [Eq. (26.58)]. Similarly, when one explores the light-cone structure for a spinning black hole in the Kerr coordinates (Fig. 26.7c,d), one finds a structure like that of Eddington-Finkelstein (Fig. 26.4a): At large radii, $r \gg M$, the light cones have their usual 45-degree form, but as one moves inward toward the

horizon, they begin to tilt inward. In addition to the inward tilt, there is a frame-dragging-induced tilt in the direction of the hole's rotation, $+\phi$. At the horizon, the outermost edge of the light cone is tangent to the horizon generators; and in Kerr coordinates, as in Boyer-Lindquist, these generators rotate around the horizon with angular velocity $d\tilde{\phi}/d\tilde{t} = \Omega_H$ [cf. Eq. (26.73), which says that at fixed r, $\tilde{t} = t + \text{constant}$ and $\tilde{\phi} = \phi + \text{constant}$].

This light-cone structure demonstrates graphically that the horizon is at the radius $r = r_H$. Outside there, the outer edge of the light cone tilts toward increasing r and so it is possible to escape to radial infinity. Inside there the outer edge of the light cone tilts inward, and all forms of matter and energy are forced to move inward, toward a singularity whose structure, presumably, is governed by the laws of quantum gravity.[5]

26.5.4 Evolution of Black Holes — Rotational Energy and Its Extraction

When a spinning star collapses to form a black hole, its centrifugal forces will flatten it, and the dynamical growth of flattening will produce gravitational radiation (Chap. 27). The newborn hole will also be flattened and will not have the Kerr shape; but rather quickly, within a time $\Delta t \sim 10$'s or 100's of $M \sim 10\mu s\,(M/M_\odot)$, the deformed hole will shake off its deformations as gravitational waves and settle down into the Kerr shape. This is the conclusion of extensive analyses, both analytic and numerical.

Many black holes are in binary orbits with stellar companions, and pull gas off their companions and swallow it. Other black holes accrete gas from interstellar space. Any such accretion causes the hole's mass and spin to evolve in accord with the conservation laws (25.93) and (25.94). One might have thought that by accreting a large amount of angular momentum, a hole's angular momentum per unit mass a could grow larger than its mass M. If this were to happen, then $r_H = M + \sqrt{M^2 - a^2}$ would cease to be a real radius—a fact that signals the destruction of the hole's horizon: As a grows to exceed M, the inward light-cone tilt gets reduced so that everywhere the outer edge of the cone points toward increasing r, which means that light, particles, and information are no longer trapped.

Remarkably, however, it appears that the laws of general relativity forbid a ever to grow larger than M. As accretion pushes a/M upward toward unity, the increasing drag of inertial frames causes a big increase of the hole's cross section to capture material with negative angular momentum (which will spin the hole down) and a growing resistance to capturing any further material with large positive angular momentum. Infalling particles that might try to push a/M over the limit get flung back out by huge centrifugal forces, before they can reach the horizon. A black hole, it appears, is totally resistant against having its horizon destroyed.

In 1969, Roger Penrose discovered that a large fraction of the mass of a spinning black hole is in the form of rotational energy, stored in the whirling spacetime curvature outside

---

[5]Much hoopla has been made of the fact that in the Kerr spacetime it is possible to travel inward, through a "Cauchy horizon" and then into another universe. However, the Cauchy horizon, located at $r = M - \sqrt{M^2 - a^2}$ is highly unstable against perturbations, which convert it into a singularity with infinte spacetime curvature. For details of this instability and the singularity, see, e.g., Brady, Droz and Morsink (1998) and references therein.

the hole's horizon; and this rotational energy can be extracted. Penrose discovered this by the following thought experiment:

From far outside the hole, you throw a massive particle into the vicinity of the hole's horizon. Assuming you are at rest with respect to the hole, your 4-velocity is $\vec{U} = \partial/\partial t$. Denote by $E^{\mathrm{in}} = -\vec{p}^{\,\mathrm{in}} \cdot \vec{U} = -\vec{p}^{\,\mathrm{in}} \cdot (\partial/\partial t) = -p_t^{\mathrm{in}}$ the energy of the particle (rest mass plus kinetic), as measured by you; cf. Eq. (2.30). As the particle falls, p_t^{in} is conserved because of the Kerr metric's time-translation symmetry. Arrange that, as the particle nears the horizon, it splits into two particles, one (labeled "plunge") plunges through the horizon and the other (labeled "out") flies back out to large radii, where you catch it. Denote by $E^{\mathrm{plunge}} \equiv -p_t^{\mathrm{plunge}}$ the conserved energy of the plunging particle and by $E^{\mathrm{out}} \equiv -p_t^{\mathrm{out}}$ that of the out-flying particle. Four-momentum conservation at the event of the split dictates that $\vec{p}^{\,\mathrm{in}} = \vec{p}^{\,\mathrm{plunge}} + \vec{p}^{\,\mathrm{out}}$, which implies this same conservation law for all the components of the 4-momenta, in particular

$$E^{\mathrm{out}} = E^{\mathrm{in}} - E^{\mathrm{plunge}} . \tag{26.75}$$

Now, it is a remarkable fact that the Boyer-Lindquist time basis vector $\partial/\partial t$ has a squared length $\partial/\partial t \cdot \partial/\partial t = g_{tt} = -\alpha^2 + \varpi^2 \omega^2$ that becomes positive (so $\partial/\partial t$ becomes spacelike) at radii

$$\boxed{r < r_{\mathrm{ergo}} \equiv M + \sqrt{M^2 - a^2 \cos^2 \theta}} . \tag{26.76}$$

Notice that r_{ergo} is larger than r_H everywhere except on the hole's spin axis, $\theta = 0, \pi$. The region $r_H < r < r_{\mathrm{ergo}}$ is called the hole's *ergosphere*. If the split into two particles occurs in the ergosphere, then it is possible to arrange the split such that the scalar product of the *timelike* vector $\vec{p}^{\,\mathrm{plunge}}$ with the *spacelike* vector $\partial/\partial t$ is *positive*, which means that the plunging particle's conserved energy $E^{\mathrm{plunge}} = -\vec{p}^{\,\mathrm{plunge}} \cdot (\partial/\partial t)$ is *negative*; whence [by Eq. (26.75)]

$$E^{\mathrm{out}} > E^{\mathrm{in}} . \tag{26.77}$$

see Ex. 26.13a.

When the outflying particle reaches your location, $r \gg M$, its conserved energy is equal to its physically measured total energy (rest-mass plus kinetic); and the fact that $E^{\mathrm{out}} > E^{\mathrm{in}}$ means that you get back more energy (rest-mass plus kinetic) than you put in. The hole's asymptotic energy-conservation law (25.93) implies that the hole's mass has decreased by precisely the amount of energy that you have extracted,

$$\Delta M = -(E^{\mathrm{out}} - E^{\mathrm{in}}) = E^{\mathrm{plunge}} < 0 . \tag{26.78}$$

A closer scrutiny of this process (Ex. 26.13f) reveals that the plunging particle must have had negative angular momentum, so it has spun the hole down a bit. The energy you extracted, in fact, came from the hole's enormous store of rotational energy, which makes up part of its mass M; and your extraction of energy has reduced that rotational energy.

Stephen Hawking has used sophisticated mathematical techniques to prove that, independently of how you carry out this thought experiment, and, indeed, independently of what is done to a black hole, general relativity requires that the horizon's surface area A_H never decrease. This is called the *second law of black-hole mechanics*, and it actually turns out to be

a variant of the second law of thermodynamics, in disguise (Ex. 26.13g). A straightforward calculation (Ex. 26.12) reveals that the horizon surface area is given by

$$\boxed{A_H = 4\pi(r_H^2 + a^2) = 8\pi M r_H \quad \text{for a spinning hole}} , \qquad (26.79\text{a})$$

$$\boxed{A_H = 16\pi M^2 \quad \text{for a nonspinning hole, } a = 0} . \qquad (26.79\text{b})$$

Dimitrious Christodoulou has shown (cf. Ex. 26.13) that, in the Penrose process, the non-decrease of A_H is the only constraint on how much energy one can extract, so by a sequence of optimally designed particle injections and splits that keep A_H unchanged, one can reduce the mass of the hole to

$$\boxed{M_{\text{irr}} = \sqrt{\frac{A_H}{16\pi}} = \sqrt{\frac{M(M + \sqrt{M^2 - a^2})}{2}}} , \qquad (26.80)$$

but no smaller. This is called the hole's irreducible mass. The hole's total mass is the sum of its irreducible mass and its rotational energy M_{rot}; so the rotational energy is

$$\boxed{M_{\text{rot}} = M - M_{\text{irr}} = M \left[1 - \sqrt{\frac{1}{2}\left(1 + \sqrt{1 - a^2/M^2}\right)}\right]} . \qquad (26.81)$$

For the fastest possible spin, $a = M$, this gives $M_{\text{rot}} = M(1 - 1/\sqrt{2}) \simeq 0.2929M$. This is the maximum amount of energy that can be extracted, and it is enormous compared to the energy $\sim 0.005M$ that can be released by thermonuclear burning in a star with mass M.

The Penrose process of throwing in particles and splitting them in two is highly idealized, and of little or no importance in Nature. However, Nature seems to have found a very effective method for extracting rotational energy from spinning black holes: the *Blandford-Znajek (1977) process* in which magnetic fields, threading through a black hole and held on the hole by a surrounding disk of hot plasma, extract energy electromagnetically. This process is thought to power the gigantic jets that shoot out of the nuclei of some galaxies, and might also be the engine for some powerful gamma-ray bursts.

****

EXERCISES

Exercise 26.12 *Derivation: Surface Area of a Spinning Black Hole*
From the Kerr metric (26.66) derive Eq. (26.79) for the surface area of a spinning black hole's horizon—i.e., the surface area of the two-dimensional surface $\{r = r_H,\ t = \text{constant}\}$.

Exercise 26.13 ***Example: Penrose Process, Hawking Radiation, and Thermodynamics of Black Holes*

(a) Consider the Penrose process, described in the text, in which a particle flying inward toward a spinning hole's horizon splits in two inside the ergosphere, and one piece plunges into the hole while the other flies back out. Show that it is always possible to arrange this process so the plunging particle has negative energy, $E^{\text{plunge}} = -\vec{p}^{\text{plunge}} \cdot \partial/\partial t < 0$. [Hint: Perform a calculation in a local Lorentz frame in which $\partial/\partial t$ points along a spatial basis vector, $\vec{e}_{\hat{1}}$. Why is it possible to find such a local Lorentz frame?]

(b) Around a spinning black hole consider the vector field

$$\vec{\xi}_H \equiv \partial/\partial t + \Omega_H \partial/\partial \phi \,, \tag{26.82}$$

where Ω_H is the Horizon's angular velocity. Show that in the horizon (at radius $r = r_H$) this vector field is null and is tangent to the horizon generators. Show that all other vectors in the horizon are spacelike.

(c) In the Penrose process, the plunging particle changes the hole's mass by an amount ΔM and its spin angular momentum by an amount ΔJ_H. Show that

$$\Delta M - \Omega_H \Delta J_H = -\vec{p}^{\text{plunge}} \cdot \vec{\xi}_H \,. \tag{26.83}$$

Here $\vec{p}^{\text{plunge}}$ and $\vec{\xi}_H$ are to be evaluated at the event where the particle plunges through the horizon, so they both reside in the same tangent space. [Hint: the angular momentum carried into the horizon is the quantity $p_\phi^{\text{plunge}} = \vec{p}^{\text{plunge}} \cdot \partial/\partial \phi$. Why? This quantity is conserved along the plunging particle's world line. Why?]

(d) Show that if $\vec{A}$ is any future directed timelike vector and $\vec{K}$ is any null vector, both living in the tangent space at the same event in spacetime, then $\vec{A} \cdot \vec{K} < 0$. [Hint: Perform a calculation in a specially chosen local Lorentz frame.] Thereby conclude that $-\vec{p}^{\text{plunge}} \cdot \vec{\xi}_H$ is positive, whatever may be the world line and rest mass of the plunging particle.

(e) Show that, in order for the plunging particle to decrease the hole's mass, it must also decrease the hole's angular momentum; i.e., it must spin the hole down a bit.

(f) Hawking's second law of black-hole mechanics says that, whatever may be the particle's world line and rest mass, when the particle plunges through the horizon it causes the horizon's surface area A_H to increase. This suggests that the always positive quantity $\Delta M - \Omega_H \Delta J_H = -\vec{p}^{\text{plunge}} \cdot \vec{\xi}_H$ might be a multiple of the increase ΔA_H of the horizon area. Show that this is, indeed, the case:

$$\boxed{\Delta M = \Omega_H \Delta J_H + \frac{g_H}{8\pi} \Delta A_H}\,, \tag{26.84}$$

where g_H is given in terms of the hole's mass M and the radius r_H of its horizon by

$$\boxed{g_H = \frac{r_H - M}{2Mr_H}}\,. \tag{26.85}$$

[You might want to do the algebra, based on Kerr-metric formulae, on a computer.] The quantity g_H is called the hole's "surface gravity" for a variety of reasons, including the fact that an observer who hovers just above a horizon generator, blasting his or her rocket engines to avoid falling into the hole, has a 4-acceleration with magnitude g_H/α and thus feels a "gravitational acceleration" of this magnitude; here $\alpha = g^{tt}$ is a component of the Kerr metric called the *lapse function*, Eqs. (26.65a) and (26.67). This gravitational acceleration is arbitrarily large for an observer arbitrarily close to the horizon (where Δ and hence α is arbitrarily close to zero); when renormalized by α to make it finite, the acceleration is g_H. Equation (26.84) is called the first law of black-hole mechanics because of its resemblance to the first law of thermodynamics.

(g) Stephen Hawking has shown, using quantum field theory, that a black hole's horizon emits thermal (black-body) radiation. The temperature of this "Hawking radiation", as measured by the observer who hovers just above the horizon, is proportional to the gravitational acceleration g_H/α that the observer measures, with a proportionality constant $\hbar/2\pi k_B$, where $\hbar$ is Planck's constant and k_B is Boltzmann's constant. As this thermal radiation climbs out of the horizon's vicinity and flies off to large radii, its frequencies and temperature get redshifted by the factor α, so as measured by distant observers the temperature is

$$T_H = \frac{\hbar}{2\pi k_B} g_H \,. \tag{26.86}$$

This suggests a reinterpretation of the first law of black-hole mechanics (26.84) as the first law of thermodynamics for a black hole:

$$\Delta M = \Omega_H \Delta J_H + T_H \Delta S_H \,, \tag{26.87}$$

where S_H is the hole's entropy; cf. Eq. (4.61). Show that this entropy is related to the horizon's surface area by

$$S_H = k_B \frac{A_H}{4\ell_p^2} \,, \tag{26.88}$$

where $\ell_p = \sqrt{\hbar G/c^3} = 1.616 \times 10^{-33}$ cm is the Planck length (with G Newton's gravitation constant and c the speed of light). Because $S_H \propto A_H$, the second law of black-hole mechanics is actually the second law of thermodynamics in disguise. A black hole's entropy always increases. [Actually, the emission of the Hawking radiation will decrease the hole's entropy and surface area; but general relativity doesn't know about this because general relativity is a classical theory, and Hawking's prediction of the thermal radiation is based on quantum theory. Thus, the Hawking radiation violates the second law of black hole mechanics. It does not, however, violate the second law of thermodynamics, because the entropy carried into the surrounding universe by the Hawking radiation exceeds the magnitude of the decrease of the hole's entropy. The total entropy of hole plus universe increases.]

(h) For a ten solar mass, nonspinning black hole, what is the temperature of the Hawking radiation in degrees Kelvin, and what is the hole's entropy in units of the Boltzmann constant?

(i) Reread the discussions of black-hole thermodynamics and entropy in the expanding universe in Secs. 4.10.2 and 4.10.3, which rely on the results of this exercise.

****

26.6 ⬚T2⬚ The Many-Fingered Nature of Time

We conclude this chapter with a discussion of a concept which John Archibald Wheeler (the person who has most clarified the conceptual underpinnings of general relativity) calls the *many-fingered nature of time*.

In the flat spacetime of special relativity there are preferred families of observers: Each such family lives in a global Lorentz reference frame and uses that frame to split spacetime into space plus time. The hypersurfaces of constant time ("slices of simultaneity") which result from that split are flat hypersurfaces which slice through all of spacetime (Fig. 26.8a). Of course, different preferred families live in different global Lorentz frames and thus split up spacetime into space plus time in different manners (e.g., the dotted and dashed slices of constant time in Fig. 26.8a as contrasted to the solid ones). As a result, there is no universal concept of time in special relativity; but, at least, there are some strong restrictions on time: Each inertial family of observers will agree that another family's slices of simultaneity are flat slices.

In general relativity, i.e., in curved spacetime, even this restriction is gone: In a generic curved spacetime there are no flat hypersurfaces, and hence no candidates for flat slices
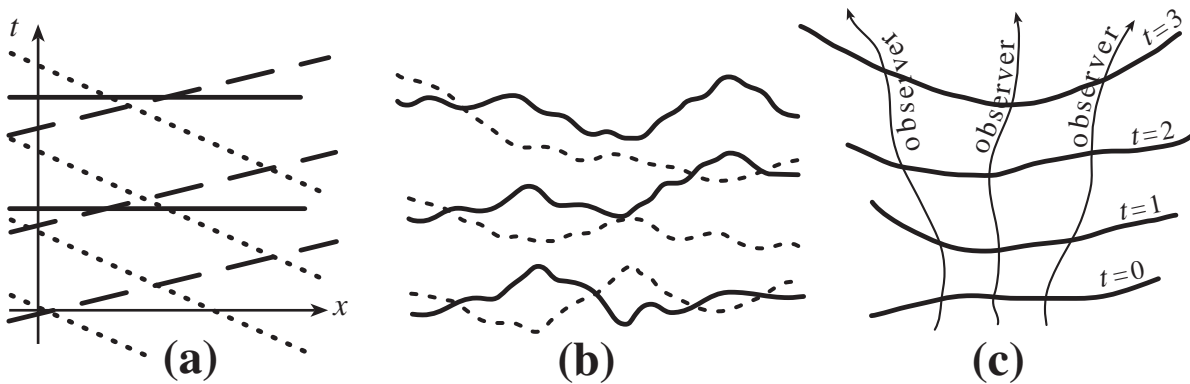
Fig. 26.8: Spacetime diagrams showing the slices of simultaneity as defined by various families of observers. Diagram (a) is in flat spacetime, and the three families (those with solid slices, those with dashed, and those with dotted) are inertial, so their slices of constant time are those of global Lorentz frames. Diagram (b) is in curved spacetime, and the two families' slices of simultaneity illustrate the "many fingered" nature of time. Diagram (c) illustrates the selection of an arbitrary foliation of spacelike hypersurfaces of simultaneity, and the subsequent construction of the world lines of observers who move orthogonal to those hypersurfaces, i.e., for whom light-ray synchronization will define those hypersurfaces as simultaneities.

of simultaneity. Hand in hand with this goes the fact that, in a generic curved spacetime there are no global Lorentz frames, and thus no preferred families of observers. A family of observers who are all initially at rest with respect to each other, and each of whom moves freely (inertially), will soon acquire relative motion because of tidal forces. As a result, their slices of simultaneity (defined locally by Einstein light-ray synchronization, and then defined globally by patching together the little local bits of slices) may soon become rather contorted. Correspondingly, as is shown in Fig. 26.8b, different families of observers will slice spacetime up into space plus time in manners that can be quite distorted, relative to each other—with "fingers" of one family's time slices pushing forward, ahead of the other family's here, and lagging behind there, and pushing ahead in some other place.

In curved spacetime it is best to not even restrict oneself to inertial (freely falling) observers. For example, in the spacetime of a static star, or of the exterior of a Schwarzschild black hole, the family of static observers [observers whose world lines are $\{(r, \theta, \phi) = \text{const}$, t varying}] are particularly simple; their world lines mold themselves to the static structure of spacetime in a simple, static manner. However, these observers are not inertial; they do not fall freely. This need not prevent us from using them to split up spacetime into space plus time, however. Their proper reference frames produce a perfectly good split; and when one uses that split, in the case of a black hole, one obtains a 3-dimensional-space version of the laws of black-hole physics which is a useful tool in astrophysical research; see Thorne, Price, and Macdonald (1986).

For any family of observers, accelerated or inertial, the slices of simultaneity as defined by Einstein light-ray synchronization over small distances (or equivalently by the space slices of the observer's proper reference frames) are the 3-surfaces orthogonal to the observers' world lines; cf. Fig. 26.8c. To see this most easily, pick a specific event along a specific observer's world line, and study the slice of simultaneity there from the viewpoint of a local Lorentz frame in which the observer is momentarily at rest. Light-ray synchronization guarantees that, locally, the observer's slice of simultaneity will be the same as that of this local Lorentz frame; and, since the frame's slice is orthogonal to its own time direction and that time direction is the same as the direction of the observer's world line, the slice is orthogonal to the observer's world line. By the discussion in Sec. 23.5, the slice is also the same, locally (to first order in distance away from the world line), as a slice of constant time in the observer's proper reference frame.

If the observers rotate around each other (in curved spacetime or in flat), it is not be possible to mesh their local slices of simultaneity, defined in this manner, into global slices of simultaneity; i.e., there are no global 3-dimensional hypersurfaces orthogonal to their world lines. We can protect against this eventuality by choosing the slices first: Select any family of non-intersecting spacelike slices through the curved spacetime (Fig. 26.8c). Then there will be a family of timelike world lines that are everywhere orthogonal to these hypersurfaces. A family of observers who move along those orthogonal world lines and who define their 3-spaces of simultaneity by local light-ray synchronization will thereby identify the orthogonal hypersurfaces as their simultaneities. Ex. 26.14 illustrates these ideas using Schwarzschild spacetime, and Box 26.3 uses these ideas to visualize a black hole's spacetime curvature.

Box 26.3

T2 Tendex and Vortex Lines Outside a Black Hole

When one uses a family of spacelike slices, with unit normals (4-velocities of orthogonally moving observers) $\vec{w}$, to split spacetime up into space plus time, the electromagnetic field tensor **F** gets split up into the electric field $E^\alpha = F^{\alpha\beta} w_\beta$ and the magnetic field $B^\beta = \frac{1}{2} \epsilon^{\alpha\beta\gamma\delta} F_{\gamma\delta} w_\delta$. These are 3-vectors lying in the spacelike slices. In terms of components in the observers' proper reference frames, these fields are $E^{\hat{j}} = F^{\hat{0}\hat{j}}$ and $B^{\hat{i}} = \epsilon^{\hat{i}\hat{j}\hat{k}} F_{\hat{j}\hat{k}}$. See Sec. 2.11 and especially Fig. 2.10. Similarly, the foliation splits the vacuum Riemann tensor into the symmetric, trace-free *tidal field* $\mathcal{E}_{\hat{i}\hat{j}} = R_{\hat{i}\hat{0}\hat{j}\hat{0}}$ (which produces relative accelerations $\Delta a_{\hat{i}} = -\mathcal{E}_{\hat{i}\hat{j}} \xi^{\hat{j}}$ of particles separated by $\xi^{\hat{j}}$), and the *frame-drag field* $\mathcal{B}_{\hat{i}\hat{j}} = \frac{1}{2} \epsilon_{\hat{i}\hat{p}\hat{q}} R^{\hat{p}\hat{q}}{}_{\hat{j}\hat{0}}$ (which produces differential frame dragging $\Delta\Omega_{\hat{i}} = \mathcal{B}_{\hat{i}\hat{j}} \xi^{\hat{j}}$). See Box 25.2.

Just as the electromagnetic field can be visualized using electric and magnetic field lines that live in the spacelike slices, so also the tidal field and frame-drag field can each be visualized using integral curves of its three eigenvector fields: the tidal field's *tendex lines* and the frame-drag field's *vortex lines* (Box 25.2). These lines lie in the space slices and are often color coded by their eigenvalues, which are called the lines' *tendicities* and *(frame-drag) vorticities.*

For a non-spinning (Schwarzschild) black hole, the frame-drag field vanishes (no spin implies no frame dragging); and the tidal field (with slicing either via Schwarzschild coordinate time t or Eddington-Finklestein coordinate time $\tilde{t}$) has proper-reference-frame components $\mathcal{E}_{\hat{r}\hat{r}} = -2M/r^3$, $\mathcal{E}_{\hat{\theta}\hat{\theta}} = \mathcal{E}_{\hat{\phi}\hat{\phi}} = +M/r^3$ [Eq. (6) of Box 26.2]. This tidal field's eigenvectors are $\vec{e}_{\hat{r}}$, $\vec{e}_{\hat{\theta}}$ and $\vec{e}_{\hat{\phi}}$, and their integral curves (the tendex lines) are identical to those shown for a weakly gravitating, spherical body at the bottom left of Box 25.2.

For a black hole with large spin, $a/M = 0.95$, it is convenient to choose, as our space slices, hypersurfaces of constant Kerr coordinate time $\tilde{t}$, since these penetrate smoothly through the horizon. The tendex and vortex lines that live in those slices have the following forms (Fang et. al. 2012):

Tendex Lines
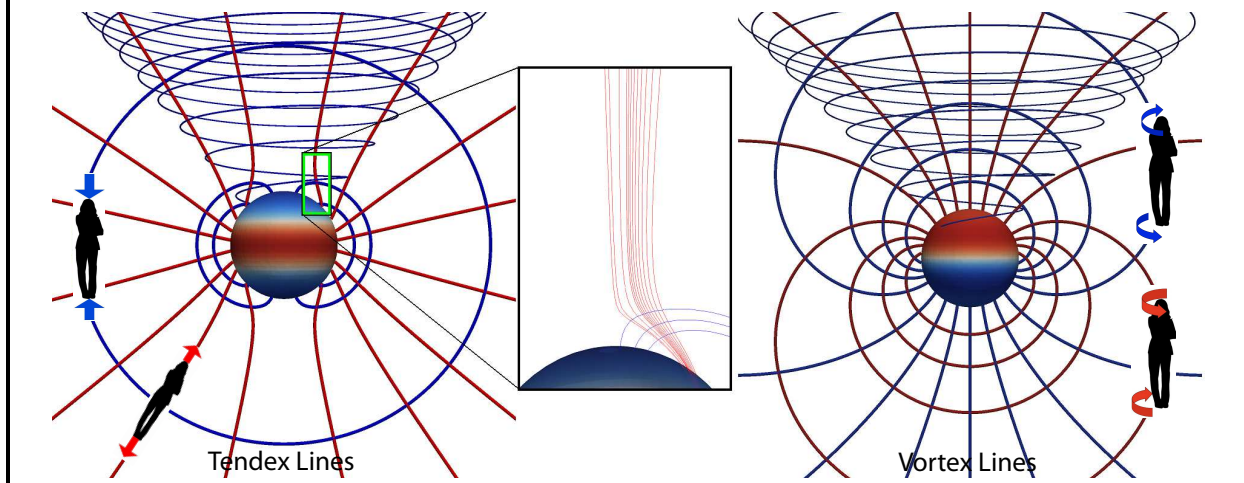
Vortex Lines

T2 **Box 25.3 (continued)**

The tendex lines are shown on the left and in the central inset; the vortex lines are shown on the right. The horizon is color coded by the sign of the tendicity (left) and vorticity (right) of the lines that emerge from it: blue for positive and red for negative.

The blue tendex lines have positive tendicity, and the tidal-acceleration equation $\Delta a_{\hat{i}} = -\mathcal{E}_{\hat{i}\hat{j}}\xi^{\hat{j}}$ says that a person whose body is oriented along them gets squeezed with relative "gravitational" acceleration between head and foot equal to their tendicity times her body length. The red lines have negative tendicity, so they stretch a person with a head-to-foot relative acceleration equal to the magnitude of their tendicity times body length. Notice that near the poles of a fast-spinning black hole, the radial tendex lines are blue , and in the equatorial region they are red. Therefore, a person falling into the polar regions of a fast-spinning hole gets squeezed radially, and one falling into the equatorial regions gets stretched radially

For a person with body oriented along a vortex line, the differential frame-drag equation $\Delta\Omega_{\hat{i}} = \mathcal{B}_{\hat{i}\hat{j}}\xi^{\hat{j}}$ says that a gyroscope at her feet precesses clockwise (blue line, positive vorticity) or counterclockwise (red line, negative vorticity) relative to inertial frames at her head. And a gyroscope at her head precesses in that same direction relative to inertial frames at her feet. Thus, the vortex lines can be regarded as either counterclockwise (red) or clockwise (blue). The precessional angular velocity is equal to the line's (frame-drag) vorticity times the person's body length.

Notice that counterclockwise (red) vortex lines emerge from the north polar region of the horizon, swing around the south pole, and descend back into the north polar region; and similarly (blue) vortex lines emerge from the horizon's south polar region, swing around the north pole, and descend back into the south. This is similar to the vortex lines for a spinning body in Linearized Theory (bottom right of Box 25.2). The differential precession is counterclockwise along the (red) near-horizon radial lines in the north polar region because gyroscopes near the horizon are dragged into precession more strongly, by the hole's spin, the nearer one is to the horizon. This also explains the clockwise precession along the (blue) near-horizon radial lines in the south polar region.

For more details about the tendex and vortex lines of Kerr black holes, see Zhang et. al. (2012).

****

EXERCISES

Exercise 26.14 *Practice: Slices of Simultaneity in Schwarzschild Spacetime*

(a) One possible choice of slices of simultaneity for Schwarzschild spacetime is the set of 3-surfaces $t = $ const, where t is the Schwarzschild time coordinate. Show that the unique family of observers for whom these are the simultaneities are the static observers, with world lines $\{(r, \theta, \phi) = $ const, t varying$\}$. Explain why these slices of simultaneity

and families of observers exist only outside the horizon of a black hole, and cannot be extended into the interior. Draw a picture of the world lines of these observers and their slices of simultaneity in an Eddington-Finkelstein spacetime diagram.

(b) A second possible choice of simultaneities is the set of 3-surfaces $\tilde{t} = $ const, where $\tilde{t}$ is the Eddington-Finkelstein time coordinate. What are the world lines of the observers for whom these are the simultaneities? Draw a picture of those world lines in an Eddington-Finkelstein spacetime diagram. Note that they and their simultaneities cover the interior of the hole as well as its exterior.

****

Bibliographic Note

In our opinion, the best elementary textbook treatment of black holes and relativistic stars is that in Chaps. 12, 13, 15, and 24 of Hartle (2003); this treatment is also remarkably complete. For nonrotating, relativistic stars at an elementary level we also recommend Chap. 10 of Schutz (1980), and at a more advanced level (including stellar pulsations), Chaps. 23, 24, and 26 of MTW. For black holes at an intermediate level see Chaps. 5 and 6 of Carroll (2004), and at a more advanced level, Chap. 12 of Wald (1984) which is brief and highly mathematical, and Chaps. 31–34 of MTW which is long and less mathematical.

The above are all portions of general relativity textbooks. There are a number of books and monographs devoted solely to the theory of black holes and/or relativistic stars. Among these, we particularly recommend the following: Shapiro and Teukolsky (1983) is an astrophysically oriented book at much the same level as this chapter, but with much greater detail and extensive applications; it deals with black holes, neutron stars and white dwarf stars in astrophysical settings. Frolov and Novikov (1998) is a very thorough monograph on black holes, including their fundamental theory, and their interactions with the rest of the universe; it includes extensive references to the original literature and readable summaries of all the important issues that had been treated by black-hole researchers as of 1997. Chandrasekhar (1983) is an idiosyncratic but elegant and complete monograph on the theory of black holes and especially small perturbations of them.

Bibliography

Bertotti, Bruno, 1959. "Uniform Electromagnetic Field in the Theory of General Relativity," *Physical Review*, **116**, 1331–1333.

Birkhoff, George, 1923. *Relativity and Modern Physics*, Harvard University Press, Cambridge, Massachusetts.

Blandford, Roger D. and Znajek, Roman L. 1977, "The Electromagnetic Extraction of Energy from Kerr Black Holes", *Monthly Notices of the Royal Astronomical Society*, **179**, 433-456.

Brady, Patrick R., Droz, S., and Morsink, Sharon M., 1998. "The late-time singularity inside non-spherical black holes," *Phys. Rev. D*, **D58**, 084034.

Carroll, S. M., 2004. *Spacetime and Geometry: An Introduction to General Relativity*, San Francisco: Addison Wesley.

Chandrasekhar, Subramahnian, 1983. *The Mathematical Theory of Black Holes*, Oxford University Press, Oxford.

Eddington, Arthur S., 22. *The Mathematical Theory of Relativity*, Cambridge University Press, Cambridge.

Finkelstein, David, 1958. "Past-future asymmetry of the gravitational field of a point particle," *Physical Review*, **110**, 965–967.

Flamm, Ludwig, 1916. "Beiträge zur Einsteinschen Gravitationstheorie," *Physik Z.*, **17**, 448–454.

Frolov, Valery Pavlovich and Novikov, Igor Dmitrievich, 1998. *The Physics of Black Holes*, second edition, Kluwer Academic Publishers, Berlin. *Physical Review D*, **42**, 1915–1930.

Fuller, Robert W. and Wheeler, John A., 1962. "Causality and Multiply Connected Spacetime", *Physical Review*, **128**, 919–929.

Hartle, J. B., 2003. *Gravity: An Introduction to Einstein's General Relativity*, San Francisco: Addison-Wesley.

Kruskal, Martin D, 1960. "The Maximal Extension of the Schwarzschild Metric," *Physical Review*, **119**, 1743–1745.

MTW: Misner, Charles W., Thorne, Kip S. and Wheeler, John A., 1973. *Gravitation*, W. H. Freeman & Co., San Francisco.

Morris, Mike and Thorne, Kip S., 1988. "Wormholes in spacetime and their use for interstellar travel: a tool for teaching general relativity," *American Journal of Physics*, **56**, 395–416.

Oppenheimer, J. Robert, and Snyder, Hartland, 1939. "On continued gravitational contraction," *Physical Review*, **56**, 455–459.

Oppenheimer, J. Robert, and Volkoff, George, 1939. "On massive neutron cores," *Physical Review*, **55**, 374–381.

Robinson, Ivor, 1959. "A Solution of the Maxwell-Einstein Equations," *Bull. Acad. Polon. Sci.*, **7**, 351–352.

Sargent, Wallace L. W., Young, Peter J., Boksenberg, A., Shortridge, Keith, Lynds, C. R., and Hartwick, F. D. A., 1978. "Dynamical evidence for a central mass condensation in the galaxy M87," *Astrophysical Journal*, **221**, 731–744.

Schutz, B. 1980. *Geometrical Methods of Mathematical Physics*, Cambridge: Cambridge University Press.

Schwarzschild, Karl, 1916a. "Über das Gravitationsfeld eines Massenpunktes nach der Einsteinschen Theorie," *Sitzungsberichte der Königlich Preussischen Akademie der Wissenschaften*, **1916 vol. I**, 189–196.

Schwarzschild, Karl, 1916b. "Über das Gravitationsfeld einer Kugel aus inkompressibler Flüssigkeit nach der Einsteinschen Theorie," *Sitzungsberichte der Königlich Preussischen Akademie der Wissenschaften*, **1916 vol. I**, 424–434.

Shapiro, Stuart L. and Teukolsky, Saul A., 1983. *Black Holes, White Dwarfs, and Neutron Stars*, Wiley, New York.

Szekeres, George, 1960. "On the Singularities of a Riemann Manifold", *Publ. Mat. Debrecen*, **7**, 285–301.

Thorne, Kip S., Price, Richard H. and Macdonald, Douglas A., 1986. *Black Holes: The Membrane Paradigm*, Yale University Press, New Haven, Conn..

Tolman, Richard Chace, 1939. "Static solutions of Einstein's field equations for spheres of fluid," *Physical Review*, **55**, 364–373.

Wald, R. M. 1984. *General Relativity*, Chicago: University of Chicago Press.

Zhang, F. et. al., 2012. "Visualizing Spacetime Curvature via Frame-Drag Vortexes and Tidal Tendexes II. Stationary Black Holes", *Physical Review D*, in press. Available at `http://xxx.lanl.gov/pdf/1208.3034.pdf`.

Box 26.4
Important Concepts in Chapter 26

- Schwarzschild spacetime geometry
    - Metric in Schwarzschild coordinates, Eq. (26.1); in isotropic coordinates, Ex. 26.3; in Eddington-Finkelstein coordinates, Eqs. (26.57, (26.58)
    - Connection coefficients and curvature tensors in Schwarzschild coordinates and in their orthonormal basis, Box 26.2

- Deducing the properties of a spacetime and the nature of the coordinates from a metric, Sec. sec:25Schwartzschild and Ex. 26.2

- Birkhoff's theorem, Sec. 26.3.1

- Relativistic stars, Sec. 26.3
    - Radius R always larger than gravitational radius $2M$, Eq. (26.15), Sec. 26.3.5
    - Metric (26.19) and stress-energy tensor (26.27)
    - Proper reference frame of fluid, Sec. 26.3.2
    - Deducing equations of structure from local energy-momentum conservation and the Einstein field equations, Secs. 26.3.3 and 26.3.4
    - Momentum conservation implies $(\rho + P)\mathbf{a} = -\boldsymbol{\nabla}P$, Sec. 26.3.3
    - Embedding Diagram, Sec. 26.3.5, Fig. 26.1, Ex. 26.7
    - Gravitational Redshift, Ex. 26.4

- Implosion of a star to form a Schwarzschild black hole, Sec. 26.4
    - To reach $R = 2M$ (horizon radius): infinite Schwarzschild coordinate time t but finite proper time τ and Eddington-Finkelstein time $\tilde{t}$, Sec. 26.4, Ex. 26.8
    - Finite tidal forces at horizon radius, Eq. (26.56)
    - Black-hole horizon: its formation and evolution, Fig. 26.6
    - Infinite tidal forces at singularity, Ex. 26.9

- Wormholes, Ex. 26.10

- Spinning black holes: the Kerr Spacetime, Sec. 26.5
    - Kerr metric: in Boyer-Lindquist coordinates, Eqs. (26.65); in Kerr coordinates, Eq. (26.74)
    - Dragging of inertial frames, Sec. 26.5.2
    - Horizon generators, Sec. 26.5.3, Fig. 26.7
    - Horizon radius r_H, Eq. (26.70); horizon angular velocity Ω_H, Eq. (26.72); horizon surface area A_H, Eqs. (26.79), horizon surface gravity g_H, Eq. (26.85)
    - Second law of black-hole mechanics and thermodynamics, Ex. 26.13
    - Hawking radiation, and black-hole temperature and entropy, Ex. 26.13
    - Rotational energy, energy extraction, ergosphere, irreducible mass, Sec. 26.5.4
    - Tendex lines and vortex lines, Box 26.3

- The many-fingered nature of time, Sec. 26.6